



**An Electrochemical Biosensor for the Detection of EpCAM-Based
Circulating Tumor Cells**

Hazim Samae

**A Thesis Submitted in Partial Fulfillment of the Requirements for the
Degree of Master of Science in Biomedical Engineering**

Prince of Songkla University

2022

Copyright of Prince of Songkla University



**An Electrochemical Biosensor for the Detection of EpCAM-Based
Circulating Tumor Cells**

Hazim Samae

**A Thesis Submitted in Partial Fulfillment of the Requirements for the
Degree of Master of Science in Biomedical Engineering**

Prince of Songkla University

2022

Copyright of Prince of Songkla University

Thesis Title An Electrochemical Biosensor for the Detection of
EpCAM-Based Circulating Tumor Cells

Author Mr. Hazim Samae

Major Program Biomedical Engineering

Major Advisor

.....
(Asst. Prof. Dr. Tonghathai Phairatana)

Co-advisor

.....
(Dr. Soracha Dechaumphai)

Examining Committee :

..... Chairperson
(Assoc. Prof. Dr. Benchaporn Lertanantawong)

..... Committee
(Assoc. Prof. Dr. Warakorn Limbut)

..... Committee
(Asst. Prof. Dr. Tonghathai Phairatana)

..... Committee
(Asst. Prof. Dr. Pasarat Khongkow)

..... Committee
(Dr. Soracha Dechaumphai)

The Graduate School, Prince of Songkla University, has approved this thesis as
partial fulfillment of the requirements for the Master of Science Degree in Biomedical Engineering

.....
(Asst. Prof. Dr. Thakerng Wongsirichot)

Acting Dean of Graduate School

This is to certify that the work here submitted is the result of the candidate's own investigations.
Due acknowledgement has been made of any assistance received.

..... Signature

(Asst. Prof. Dr. Tonghathai Phairatana)

Major Advisor

..... Signature

(Dr. Soracha Dechaumphai)

Co-advisor

..... Signature

(Mr. Hazim Samae)

Candidate

I hereby certify that this work has not been accepted in substance for any degree, and is not being currently submitted in candidature for any degree.

..... Signature

(Mr. Hazim Samae)

Candidate

ชื่อวิทยานิพนธ์	ไบโอเซนเซอร์ทางเคมีไฟฟ้าสำหรับตรวจวัดเซลล์มะเร็งในกระแสเลือดที่มีการแสดงออกของโปรตีนแอปแคม
ผู้เขียน	นายฮาซิม สาแม
สาขาวิชา	วิศวกรรมชีวการแพทย์
ปีการศึกษา	2565

บทคัดย่อ

มะเร็งเป็นสาเหตุของการเสียชีวิตเป็นอันดับสองของโลก และพบว่ามีผู้เสียชีวิตประมาณ 10 ล้านคนต่อปี โดยการเสียชีวิตส่วนใหญ่ของผู้ป่วยมะเร็งเกิดขึ้นในช่วงระยะแพร่กระจาย (metastasis) ซึ่งเป็นช่วงที่เซลล์มะเร็งมีการหลุดออกจากก้อนเนื้อมะเร็ง ไทลเวียนและแพร่กระจายไปยังส่วนต่างๆของร่างกายผู้ป่วย (circulating tumor cells) การตรวจวัดโดยใช้อิมมูโนเซนเซอร์ทางเคมีไฟฟ้าเป็นหนึ่งในวิธีที่มีสมรรถภาพสูงซึ่งสามารถให้ข้อมูลได้ทั้งในเชิงคุณภาพและปริมาณที่มีความไววิเคราะห์และความจำเพาะต่อการตรวจวัดต่อตัวอย่างเป้าหมายสูง โดยการศึกษาในครั้งนี้มีวัตถุประสงค์เพื่อพัฒนาอิมมูโนเซนเซอร์ทางเคมีไฟฟ้าสำหรับการตรวจวัดเซลล์มะเร็งที่ไทลเวียนในกระแสเลือดโดยใช้ขั้วไฟฟ้าทองชนิกสกรีนพรีนต์ โดยเคลือบพอลิอะนิลีนบนขั้วไฟฟ้าผ่านกระบวนการอิเล็กโทรพอลิเมอร์ไรเซชัน จากนั้นทำการเคลือบอนุภาคนาโนทองบนพื้นผิวของพอลิอะนิลีนผ่านกระบวนการทางเคมีไฟฟ้า โมเลกุลสเตรปตาวิดินและไบโอดีเอ็นเอแอนติบอดี ชนิด EpCAM ถูกตรึงไว้บนพื้นผิวเซนเซอร์และตรวจวัดเซลล์มะเร็งด้วยเทคนิคอิมพีแดนซ์สเปกโตรสโคปีเชิงเคมีไฟฟ้า จากผลการทดลองแสดงให้เห็นว่าการเพิ่มขึ้นของความต้านทานของการถ่ายโอนประจุไฟฟ้ามีความสอดคล้องกับการเพิ่มขึ้นของจำนวนความเข้มข้นของเซลล์มะเร็งชนิด MCF-7 ในช่วง 10^3 ถึง 10^6 เซลล์ต่อมิลลิลิตร (ค่าสัมประสิทธิ์สหสัมพันธ์ = 0.997) โดยมีขีดจำกัดของการตรวจวัด (limit of detection) ที่ 2 เซลล์ต่อมิลลิลิตร ($3S_u/b$) นอกจากนี้อิมมูโนเซนเซอร์มีความจำเพาะสูงและความสามารถในการทำซ้ำที่ดีอีกด้วย เครื่องมืออิมมูโนเซนเซอร์นี้สามารถเป็นเครื่องมือที่มีศักยภาพสูงที่มีความไววิเคราะห์และความจำเพาะต่อการตรวจวัดเซลล์มะเร็งเต้านมในระยะแรกสำหรับการพัฒนาเป็นอุปกรณ์ตรวจวัด ณ จุดดูแลผู้ป่วย.

คำสำคัญ: อิมพีแดนซ์สเปกโตรสโคปีเชิงเคมีไฟฟ้า, ตรวจวัดเซลล์มะเร็งที่ไทลเวียนในกระแสเลือด ปฏิสัมพันธ์ของพอลิอะนิลีนและอนุภาคนาโนทอง, การนำไฟฟ้าของโปรตีนสเตรปตาวิดิน.

Thesis Title	An Electrochemical Biosensor for the Detection of EpCAM-Based Circulating Tumor Cells
Author	Mr. Hazim Samae
Major Program	Biomedical Engineering
Academic Year	2022

ABSTRACT

Cancer is the second leading cause of death globally, accounting for an estimated 10 million deaths per year. Most deaths occur during metastasis stages when cancer cells are shed from the solid tumor and spread to other parts of the cancer patient's body (circulating tumor cell). An electrochemical immunosensor is a powerful analytical tool based on the specific interaction between antibody and antigen, in which the specific interaction is measured through electrical signals. This study aimed to develop an electrochemical immunosensor for circulating tumor cell detection using a screen-printed gold electrode (SPAuE). The developed immunosensor was fabricated by electropolymerized polyaniline (PANI) on the working electrode. Gold nanoparticles were then electrodeposited on PANI-modified SPAuE. Streptavidin molecules were immobilized on the PANI-modified SPAuE, followed by biotin-EpCAM antibody binding on the surface. Electrochemical measurements were performed using electrochemical impedance spectroscopy. The results showed an increase in charge transfer resistance related to an increase in MCF-7 cell concentrations in the range of 10 to 10^6 cells mL^{-1} (relative correlation coefficient = 0.997) with a detection limit (LOD) as low as 2 cells mL^{-1} ($3S_d/b$). The developed immunosensor also exhibited high selectivity and good reproducibility. The immunosensor could provide high-potential tools with sensitivity and selectivity to screen breast cancer cells in the early stage for point-of-care testing development.

Keywords: Electrochemical impedance spectroscopy, CTCs detection, Polyaniline and gold nanoparticles interaction, Conductive streptavidin protein.

ACKNOWLEDGEMENT

The completion of this thesis would be impossible without the help of many people.

I would like to express my heartfelt thanks to my advisor, Assistant Professor Dr. Tonghathai Phairatana and my co-advisor, Dr. Soracha Dechaumphai for giving me the opportunity to work on my interested field and also Assistant Professor Dr. Pasarat Khongkow for her advice and suggestion of this work.

I would like to thank Miss Kewarin Phonklam, Miss Piromya Thongkhao, and Mister Ittikon Siriyakul for their help, advice, and suggestion throughout the course of this work.

I would like to thank:

The supported grant of the Faculty of Medicine, Prince of Songkla University (MED6104081S);

Department of Biomedical Sciences and Biomedical Engineering, Faculty of Medicine, Prince of Songkla University, HatYai, Songkhla, Thailand.

Members of the Department of Biomedical Sciences and Biomedical Engineering, Faculty of Medicine, Prince of Songkla University for their help, encouragement, support, and friendship.

Most importantly, I would like to thank my family for their love and support throughout my life, in particular, my mother, my father, brother, and sister for their understanding and encouragement to complete this study.

Hazim Samae

The Relevance of the Research Work to Thailand

The purpose of this Master of Science thesis in Biomedical Engineering is the development of a novel electrochemical immunosensor based on polyaniline and gold nanoparticles for circulating tumor cell detection. The developed immunosensor, with suitable materials, can provide higher performances than the previous method, including good selectivity, good reproducibility, and a low limit of detection. This developed immunosensor can be applied to detect cancer cells in cancer patients from early metastasis.

CONTENTS

	Page
LIST OF TABLES	xi
LIST OF FIGURES	xii
LIST OF ABBREVIATIONS AND SYMBOLS	xiv
CHAPTER 1: INTRODUCTION	1
1.1 Background and rationale	1
1.2 Literature review	2
1.2.1 Cancer	2
1.2.2 CTCs detection	6
1.2.3 Biosensor	7
1.2.4 Materials	11
1.2.5 Analytical performance	14
1.3 Objective	16
1.4 Outline of research	16
CHAPTER 2: MATERIALS AND METHODS	17
2.1 Reagents	17
2.2 Apparatus	18
2.3 Immunosensor fabrication	18
2.4 Cell-culture experiment	20
2.5 MCF-7 cell dyeing	20
2.6 Fluorescence microscope detection	20
2.7 Electrochemical measurement	21
2.8 Linear range	21
2.9 Limit of detection	21
2.10 Selectivity	22
2.11 Reproducibility	22

CONTENTS (Cont.)

	Page
CHAPTER 3: RESULTS AND DISCUSSION	23
3.1 Immunosensor fabrication	23
3.1.1 Surface characterization of the AuNPs/PANI modified electrodes	23
3.1.2 Electrochemical characterization of the developed immunosensor	27
3.1.3 The effect of AuNPs on the streptavidin based immunosensor	32
3.2 Analytical performances of the developed immunosensor	35
3.2.1 Linearity and limit of detection	38
3.2.2 Selectivity	40
3.2.3 Reproducibility	41
CHAPTER 4: CONCLUSIONS	44
REFERENCES	45
VITAE	55

LIST OF TABLES

Table		Page
1	The data of SPAuE modification	30
2	A comparative performance of different modified electrode strategies for breast cancer cell detection	43

LIST OF FIGURES

Figure	Page
1.1 The techniques for detecting cancer disease through (A) tissue biopsy, (B) bone marrow biopsy, and (C) liquid biopsy.	3
1.2 Schematic of biosensor components, including biological recognition, recognition, transducers, and signal processing.	8
1.3 Equivalent circuit model for fitting the impedance spectra of Nyquist plot.	11
2.1 Schematic presentation of the process of the developed immunosensor using a SPAuE.	19
3.1 (A) electropolymerization process of aniline in 50 mM HClO ₄ in the potential range of 0.2 to 0.4 V at a scan rate of 50 mV s ⁻¹ for 10 cycles by CV technique and (B) FE-SEM image of the PANI forming layer prepared by 4 mM aniline monomer on SPAuE surface.	25
3.2 (A) the electrodeposition process with 15 cycle scans of 0.6 mM HAuCl ₄ in 0.5 M H ₂ SO ₄ to form AuNPs and (B) FE-SEM image of PANI modified SPAuE surface after AuNPS deposition.	26
3.3 Differential pulse voltammograms (DPV) showing the current responses of (a) bare SPAuE, (b) PANI/SPAuE, and (c) AuNPs/PANI/SPAuE in 10 mM [Fe(CN) ₆] ^{3-/4-} containing 10 mM phosphate buffer at pH 7.0.	27
3.4 Nyquist plot of the developed SPAuE in each step was obtained in 10 mM [Fe(CN) ₆] ^{3-/4-} containing 10 mM phosphate buffer at pH 7.0 using EIS technique in the frequency range of 10 ⁵ to 10 ⁻¹ Hz with a signal amplitude of 5 mV (5 points per decade) at (a) bare SPAuE, (b) PANI/SPAuE, (c) AuNPs/PANI/SPAuE, (d) SA/AuNPs/PANI/SPAuE, (e) b- EpCAM/SA/AuNPs/PANI/SPAuE, and (f) BSA/b-EpCAM/SA/AuNPs/PANI/SPAuE.	29
3.5 Streptavidin/polyaniline-modified SPAuE without AuNPs was detected with (A) EIS technique in the frequency range of 10 ⁵ to 10 ⁻¹ Hz with a signal amplitude of 5 mV (5 points per decade) and (B) CV technique in a potential range of -0.20 V to 0.60 V with a scan rate 50 mV/s. These processes were obtained in 10 mM [Fe(CN) ₆] ^{3-/4-} containing 10 mM phosphate buffer at pH 7.0	33

LIST OF FIGURES (Cont.)

Figure	Page
3.6	34
<p>Streptavidin/AuNPs/polyaniline modified SPAuE (the presence of AuNPs) was detected through (A) EIS technique in the frequency range of 10^5 to 10^{-1} Hz with a signal amplitude of 5 mV (5 points per decade) and (B) CV technique in a potential range of -0.20 V to 0.60 V with a scan rate 50 mV/s. These processes were obtained in 10 mM $[\text{Fe}(\text{CN})_6]^{3-/4-}$ containing 10 mM phosphate buffer at pH 7.0</p>	
3.7	36
<p>(A) EIS response of before (trace a) and after (trace b) detecting 10,000 cells/mL of MCF-7 cells, and (B) Equivalent circuit for fitting the impedance spectra of Nyquist plot.</p>	
3.8	37
<p>Microscope images of (A) the modified SPAuE with presence of MCF-7 cells on surface and B) the modified SPAuE without MCF-7 cells on surface.</p>	
3.9	38
<p>A cumulative graph illustration of EIS spectra response at various concentrations of MCF-7 cells in the range of 10 to 10^6 cells/mL. This process was achieved by detecting in the solution of 10 mM $[\text{Fe}(\text{CN})_6]^{3-/4-}$ containing 10 mM phosphate buffer pH 7.0</p>	
3.10	39
<p>The calibration curve presented linear relationship between charge transfer resistance (R_{ct}) value and logarithm value of cumulative MCF-7 cell concentrations that adapt from number of MCF-7 cell concentrations in the range of 10 to 10^5 cells/mL. The sensitivity was achieved by detecting in the solution of 10 mM $[\text{Fe}(\text{CN})_6]^{3-/4-}$ containing 10 mM phosphate buffer pH 7.0. (n=5)</p>	
3.11	41
<p>Effects of interfering on the response of the developed immunosensor to MCF-7, A2780, and MG 63 cells in 1X PBS solution at the concentration of 1,000 and 100,000 cells/mL of each type.</p>	
3.12	42
<p>Response of the five developed immunosensors to detect 100 cells/mL of MCF-7 cells in the solution of 10 mM $[\text{Fe}(\text{CN})_6]^{3-/4-}$ containing 10 mM phosphate buffer pH 7.0.</p>	

LIST OF ABBREVIATIONS AND SYMBOLS

A2780 cell	ovarian cancer cell
AuNPs	gold nanoparticles
b-EpCAM	biotin-epithelial cell adhesion molecules
BSA	bovine serum albumin
CPE	constant phase element
CTCs	circulating tumor cells
CV	cyclic voltammetry
DAPI	(4',6-diamidino-2-phenylindole)
DiD	carbocyanine dye
DPV	differential pulse voltammetry
EDC	N-(3-Dimethylaminopropyl)-N'-ethylcarbodiimide hydrochloride
EIS	electrochemical impedance spectroscopy
EMT	epithelial-mesenchymal transition
FDA	food and drug administration
FE-SEM	field emission scanning electron microscope
ISET	isolation by size of epithelial tumor cells
LOD	limit of detection
MCF-7 cell	breast cancer cell
MG 63 cell	bone cancer cell
NHS	N-Hydroxysuccinimide
PANI	polyaniline
PBS	phosphate buffer saline
DiD	lipophilic carbocyanine dyes
R_{ct}	charge transfer resistance
ΔR_{ct}	charge transfer resistance response
R_s	solution resistance
RSD	relative standard deviation

LIST OF ABBREVIATIONS AND SYMBOLS (Cont.)

SA	streptavidin
SEM	scanning electron microscope
SPAuE	screen-printed gold electrode
W	warburg impedance
$-Z''$	imaginary part of the impedance
Z'	real part of the impedance

CHAPTER 1

INTRODUCTION

1.1 Background and Rational

Cancer is a disease in which the body's control over cell growth is lost. Cancer can develop in any part of the body due to the rapid formation of abnormal cells. Furthermore, it can spread to other parts of the body by diffusing through blood or lymphatic vessels (metastasis phase), then stick on their moving location [1]. According to World Health Organization reported, cancer is the second leading cause of death worldwide which covered 10 million deaths in 2020 [1, 2]. A previous study found that 90 percent of cancer deaths were caused by the metastasis stage, in which the cancer cell has spread to other parts of the patient's body [3]. In terms of the treatment, the chances of a cancer patient surviving or being completely cured are inversely proportional to the amount of cancer cells in the patient's body. As a result, early detection of cancer patients is critical for treating cancer disease. The detection of circulating tumor cells (CTCs) can indicate the stage of cancer disease, allowing for the prediction of cancer type and the selection of the treatment drug. In addition, the detection via blood sample (liquid biopsy) is an intriguing method because of its non-invasiveness and low cost when compared to conventional biopsy. However, the challenge of this research field is dealing with a very low number of cancer cells in the blood sample around 2-3 cells/mL [4].

Currently, many technologies can be used to measure cancer cells in blood samples including isolation by size of epithelial tumor cells (ISET), which is a direct measuring method for identifying cancer disease by using a filter to screen cancer cells [5]. CellSearch technology captures cancer cells by using immunomagnetic coated with EpCAM antibody [5, 6]. Microfluidic devices have been used to capture cancer cells in blood by using structure in microchannels [7]. However, all of these techniques were used to analyze the characteristic of cancer cells using immunocytochemistry. They still have their limitations such as the requirement for another device for quantitative analysis, which results in more time and higher cost for analyzing

results. A biosensor is an alternative technology that can overcome the limitation of requiring another device to analyze results, offering rapid, specific, sensitive, and accurate [8]. Conductive materials and nanomaterials can be used as supporting materials to improve the performance of biosensors. Polyaniline is a conductive polymer with a high potential for improving sensor surface and conductivity, especially when combined with gold nanoparticles [9]. In addition, using streptavidin for strong capture with specific biorecognition can improve the sensitivity of sensors [10]. Thus, the goal of this study is to develop biosensors that can solve complex measurement problems, reducing the time and cost of detecting cancer cells.

1.2 Review of Literature

1.2.1 Cancer

Cancer is a term used to call a malignant tumor that occurs from abnormal cells in organs. Cancer is distinguished by uncontrollable abnormal cells and the ability to invade surrounding tissue (metastasis) by shedding a single cell from a solid tumor through a blood vessel, lymphatic vessel, or other openings in the body [1, 11]. Cancer formations, on the other hand, begin as normal cells and then transform into abnormal cells as a result of gene changes (mutations). Normally, the evolution of cancer cells to primary tumors arises from the development of existing cancerous tumor through the inheritance of generation to generation, it was stimulated through three factors, including 1) physical factors such as ultraviolet, ionizing radiation, etc. 2) chemical factors such as cigarette smoke, aflatoxin contaminating in food, arsenic contaminating in water, etc., and 3) biological factors such as infection of virus, bacteria, parasite, etc. [1]

Cancer disease is one of the diseases leading causes of death globally. It reported that the number of patients with cancer disease was nearly 20 million and nearly 10 million death in 2020. The cause of death from cancer disease occurred during the metastasis stage when cancer cells had spread throughout other parts of the body [12]. For the cancer treatment, the chance of cure is determined by the stage of cancer, or in other words, the number of cancer cells produced in the body. Generally, an X-ray has been used to screen internal organs and survey the solid tumors that formed on the organs (Fig. 1.1A). Later, cancer is determined through puncturing the spine, then cancer cells in the sample were detected by immunoassay (Fig. 1.1B) [13]. However, these methods

require high cost and high risk when receiving a large quantity of repeating an examination. As a result, these methods are unsuitable for the long-term monitoring of cancer cells. Liquid biopsy provides a better method than the previous method for detecting the number of cancer cells, due to blood containing various cancer cells that shedding from solid tumors and circulating in the blood vessel as shown in figure 1.1C, even though the number of cancer cells found in the blood is very low [14].

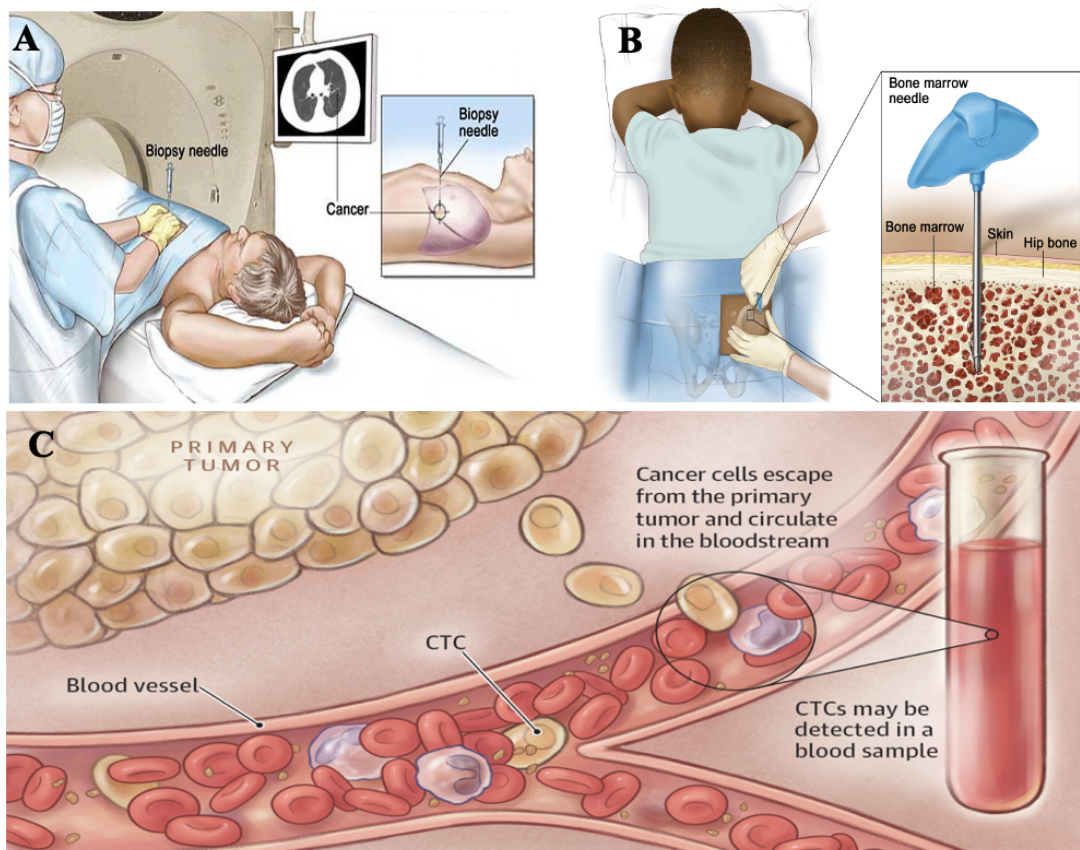


Figure 1.1 The techniques for detecting cancer disease through (A) tissue biopsy [15], (B) bone marrow biopsy [16], and (C) liquid biopsy [17].

1.2.1.1 Liquid biopsies

Tissue biopsy is widely used to diagnose various cancer diseases for determining the most appropriate treatment for each patient. However, the limitations of tissue biopsy are expensiveness, invasiveness, an inappropriate approach when repeating tests are required, and ineffectiveness to detect some types of cancer such as lung cancer due to more than 30% of lung cancer having only small cells, in which lacking a solid tumor for cancer diagnosis [18]. Moreover, cancers are quite diverse and changing all the time, leading to the previous data collection on cancer is still limited. As a result, a cancer diagnosis for treatment will be biased and will make a mistake decision. Therefore, liquid biopsy has been chosen for diagnosing cancer disease by detecting circulating tumor cells (CTCs) in the blood of cancer patients [19].

Liquid biopsy offers advantages over tissue biopsy such as no pain, inexpensive, easily accessible testing for a large population, as well as an appropriate approach for repeating tests in cancer disease stage identification or response of treatment in real-time. In addition, when a tumor is biologically evaluated in the liquid sample, it contains a lot of cancer information. There are a large number of small cancer cells that are easier to detect than tissue biopsy detection. It can be used to detect the fraction of cancer cells that remain or reappear in the body of a cancer patient [20].

The detection of biomarkers on cancer cells via liquid biopsy has gained widespread interest to diagnose cancer specialists and patients due to liquid biopsy containing the genetic information of cancer. The liquid biopsy for cancer diagnosis is divided into four types including, circulating vesicles, circulating proteins, circulating nucleic acids, and circulating tumor cells (CTCs). Circulating vesicle has been revealed that contains a lot of vesicles released from tumor tissue around 10^8 – 10^9 vesicles/mL. However, vesicles of non-cancer tumors can be also released, leading to these detection types being vague for the biomarker for cancer analysis. Circulating protein detection is used by coupling with other investigations for characteristic analysis of cancer diseases. For circulating nucleic acids, the opportunity to discover the circulating nucleic acid fragment of cancer cells is less than 1%, and in some cases lower than 0.01% of total DNA in the blood patient sample [21, 22]. Potentially, cancer detection based on circulating tumor cells is believed that it is suitable to use as a biomarker for identifying cancer disease. Despite the

fact that 2-3 circulating tumor cells (CTCs) are rarely found in 1 mL of a cancer patient's blood sample, which is mixed with 10 million white blood cells and 5 billion red blood cells [23].

1.2.1.2 Circulating tumor cells

Circulating tumor cells (CTCs) are cancer cells that have separated from the primary tumor and entered a blood vessel before circulating in the bloodstream [24]. The release of cancer cells relates to the mechanical force of contractile actomyosin protein (actin and myosin). Cell adhesion protein is then decomposed by protease (cysteine protease and matrix protease) [25, 26]. When cancer cells are released from the outer surface of a primary tumor (extracellular matrix), they can adapt to survive and protect themselves from the induction of programmed cell death (apoptosis) that occurs in normal cells. Cancer cells are adapted by modifying the function of an enzyme via a signaling format similar to that used to induce apoptosis. Cancer cells are transformed from epithelial to mesenchymal through the EMT (epithelial-mesenchymal transition) process, resulting in polarity loss. The polarity loss can reduce basement membrane binding capacity and cell-cell adhesion, allowing cells to move into other organs [25]. This avoidance of the apoptosis process allowed cancer cells to be free from the apoptosis cycle and prevented the process of eliminating cells from growing up in another organ. Later, cancer cells that have evaded apoptosis will circulate in the bloodstream until the most appropriate moment to embed in tissue arrives. As a result, it evolved into a secondary tumor cell that can be found in locations far from the original tumor location.

A biomarker on the surface of a cancer cell can be used to investigate or predict the type of cancer. It is critical to identify the type of drug used in cancer treatment. Therefore, CTCs are used to monitor cancer disease, which can reduce the severity of detection in cancer patients. However, there are challenges in developing a device for cancer detection because CTCs are extremely rare, with only 2-3 cells found in 1 mL of blood mixed with 10 million leukocytes and 5 billion erythrocytes cells [14].

1.2.2 CTCs detection

In the early stage of cancer patients, CTCs have been found around 2–3 cells per 1 mL in blood sample, which remains a big challenge for screening and measuring. CTCs have been studied in isolation and measurement through many technologies including;

1.2.2.1 Commercial device

CellSearch system is one of the advanced technologies for cancer diagnosis which is accepted by the Food and Drug Administration (FDA). Currently, it has been considered as a gold standard for enumerating CTCs in cancer diagnosis by using antibodies against the epithelial cell adhesion molecule (EpCAM) for CTC enrichment. CTCs are detected using the CellSearch system in the whole blood sample of cancer patients [27]. If the CTCs are present, they can be isolated and characterized for the management of cancer patients. In the detection of the CellSearch system, immunomagnetic was coated with a specific antibody for capturing breast cancer cells in 7.5 mL of a blood sample. After that, the breast cancer cells captured with immunomagnetic were analyzed with fluorescent dyeing by using DAPI dye (4',6-diamidino-2-phenylindole) via a nucleus inside the cancer cell. The results were shown in the form of positive for epithelial cells (cytokeratin 8, 18, 19) and negative for inactivating leukocytes (CD 45) [5]. Although this technique is a high impact on predicting EpCAM-positive CTCs, EpCAM-negative CTCs are still missing detection [28].

1.2.2.2 Research progress

Isolation by size of epithelial tumor cells (ISET) is a direct measuring method for identifying cancer cells using a filter to isolate a large size of cancer cells. Briefly, the amount of 10 mL blood sample has been diluted in an erythrocyte-lysis buffer solution with a ratio of 1 to 10 before filtering cancer cells with the ISET filter. However, this technique has been performed for 4 hours. Finally, cancer cells were stained on the filter for morphological test and reconfirming the result of characteristic cancer cells that display through immunocytochemistry [5].

Microfluidic technology for cancer cell isolation and measurement in blood samples has been developed. It is a practical possibility for detecting through the liquid sample under microscale volume and increasing the chances of cancer cell detection. This technology uses polymer to create structure on silicon or glass material offering several advantages such as reducing cost, easier fabrication, and non-toxicity [29]. The important components of microfluidic devices for detecting cancer cells in blood samples include common structure and surface modification in

the microchannel. The structural design in the microchannel is used for enhancing the efficiency of isolating and measuring cancer cells such as micro-posts for increasing surface in the microchannel or herringbone structure for transforming fluid flow from laminar to turbulent flow [30, 31]. The surface in the microchannel was modified by coating it with specific antibodies on its surface. Then cancer cells captured onto the microchannel surface were stained using fluorescent dyes for qualitative and quantitative analysis.

However, devices from the commerce and the research progress have several limitations such as requiring fluorescent dye, spending a long time, the need for additional equipment, and high cost for sample analysis. Therefore, a biosensor as an alternative technology has many great advantages to develop as an analytical device for addressing those problems. It offers high accuracy, high selectivity, no need for additional equipment, short time analysis, low cost, ease to use, and portability [32].

1.2.3 Biosensor

A Biosensor is an analytical device used for detecting a chemical substance or biomolecule in a wide range of applications such as pharmaceutical medicine, food, and environmental field [33]. The main components of biosensor consist of biological recognition and physicochemical transducer (Fig. 1.2). A biological recognition material provides specificity of biosensor to selective nature by biological interaction. A physicochemical transducer transforms the biochemical signal into a quantitative electronic signal. Biosensors can be classified based on transducer (electrochemical, optical, thermal, and piezoelectric biosensors) and based on the type of biological recognition (molecularly imprinted polymer, enzymes, nucleic acid, aptamer, antigen or antibody, whole cell, tissue, and organelle-based biosensors) [34, 35]. Biosensors are becoming an interesting tool due to offering high sensitivity, high selectivity, rapidity, ease-of-use, low cost, and portable devices [32].

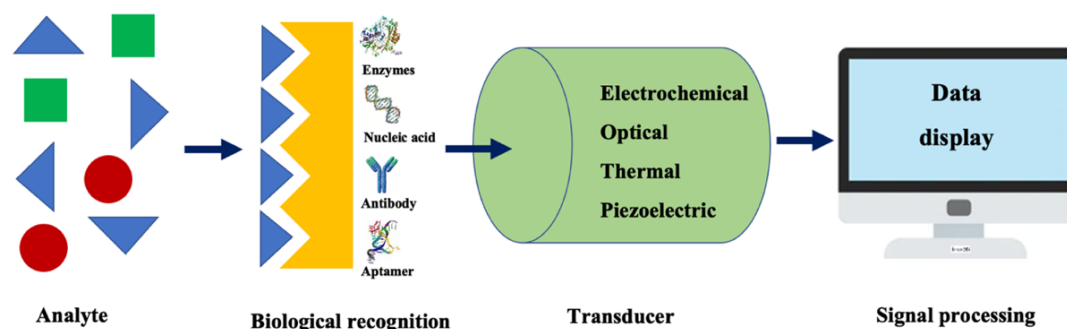


Figure 1.2 Schematic of biosensor components, including biological recognition, transducers, and signal processing.

1.2.3.1 Immunosensor

An immunosensor is an attractive biological sensor based on the specific interaction of antibody-antigen with high selectivity and sensitivity [36]. Immunoglobulin also known as antibody, is a biological recognition protein, which responds to its antigen with very strong affinity and high selectivity like a lock and key. The specific binding of antibody to antigen targets is the key point for biosensor fabrication [37].

In the principle of an immunosensor, when target antigens are captured by its specific antibody with stable immunocomplex formation on the immunosensor, the interaction of antigens and antibodies is detected and transformed to a signal by a transducing system. Different types of signal generation such as electrochemical, optical, and piezoelectric are utilized in immunological biosensors for several applications in different fields [38]. Especially, electrochemical immunosensors are powerful tools with high sensitivity and selectivity for target analyte detection. Moreover, they offer simple, real-time analysis, low-cost, portable devices, and short-time analysis [39].

1.2.3.2 Immunosensor for CTCs detection

The assay of electrochemical immunosensors can be divided into two assays. Firstly, a direct immunoassay (labeled-free immunosensor) detects the changes of physical or chemical interaction occurring directly from immunocomplex formation between antibody and antigen. However, it encounters small interferent signals from non-specific adsorption on the substrate surface that occurs when other proteins are present in the sample. Therefore, blocking

reactive free area is necessary for this direct detection assay. The other assay is an indirect immunoassay (labeled immunosensor), which is used to detect the antigen-antibody interaction based on signal generation from the labeling attached to the antigen targets or the second probe antibodies. The labeling allows an electron transfer and then interprets the signal from the number of labeling being proportional to the amount of target analytes. The advantages of labeled assays are higher sensitivity and a small effect from non-specific adsorption on the signal. However, the variability of a labeled biomolecule affects antigen-antibody binding efficiency. Furthermore, the labeling method requires time consumption, high cost, and sample preparation [40, 41].

1.2.3.3 Electrochemical techniques

1) Cyclic voltammetry

Cyclic voltammetry (CV) is an electrochemical technique that can provide both qualitative and quantitative information for investigating the electrochemical reactions of biosensor systems. The CV result reveals the information of equilibrium between reduction and oxidation reaction in the form of a cyclic voltammogram, which consists of the x-axis representing the range of applied potential and the y-axis representing the resulting current [42]. For sensor modification, CV can be used to modify an electrode with supporting materials such as conducting polymers and nanomaterials through the electrosynthesis process, and also can be used to characterize the surface of the electrode during the modification step [43, 44, 45]. There are several advantages to electrosynthesis via CV, including improved material adhesion on the electrode surface, faster synthesis, and the ability to control both the thickness of the modified layer and the morphology of material [46].

2) Differential pulse voltammetry

Differential pulse voltammetry (DPV) is a technique of electrochemistry that can be used for assessing the redox properties without background current (no faradaic reaction) [47]. In the principle, the current is measured as a function of time and applied potentials that are varied using pulses of increasing amplitude, and the current is sampled before and after each change of potential [48]. The advantage of the DPV technique is low capacitive current that leads to enhance sensitivity for analyzing with voltametric method. Therefore, DPV can be used for quantitative analysis target and less for qualitative analysis of electrode mechanisms [48]. In this work,

this technique provided us to study the success of material modification on the electrode surface and also it coupled with electrochemical impedance spectroscopy technique.

3) *Electrochemical impedance spectroscopy*

Electrochemical impedance spectroscopy (EIS) is an electrochemical technique that can be employed for analyzing electrical properties of modified electrode surfaces, and the changes in bulk properties [49]. The principle of electrochemical impedance spectroscopy measurement is based on applying AC voltage with small amplitude and measuring the current response. In other words, impedance (Z) is the quotient of voltage at time $V(t)$ and response current signal at time $I(t)$, as shown in equation 1.

$$Z = \frac{V(t)}{I(t)} = \frac{V_0 \sin(2\pi ft)}{I_0 \sin(2\pi ft + \varphi)} \quad (1)$$

where V_0 and I_0 are amplitude of the optimum voltage and current signals, f is the frequency, t is the time, and φ is the phase shift between the voltage at time and current at time [49, 50].

Furthermore, EIS measurements are performed on the conductivity of electrolyte solution as a system component. Figure 1.3 depicts some of the elements that are commonly used to explain the behavior of a sensor system. It consists of electrolyte solution resistance (R_s), charge transfer resistance (R_{ct}), a pure capacitor (C_{dl}), and Warburg impedance (Z_w). The results of electrochemical impedance spectroscopy are presented in Nyquist diagram with the imaginary part of the impedance ($-Z''$) at the y-axis versus the real part of the impedance (Z') at the x-axis and a bode plot to present all information that is visible [40].

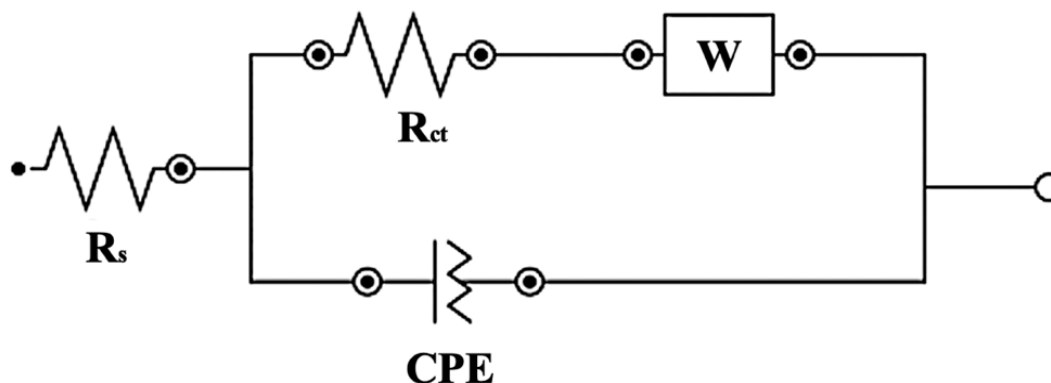


Figure 1.3 Equivalent circuit model for fitting the impedance spectra of Nyquist plot.

EIS can be used to monitor several cases such as the roughness of the electrode surface, confirmation of material immobilization on the sensor surface, and the detection of interesting analytes. EIS is very sensitive to surface electrode changes, and it can read the result directly from the Nyquist plot. As a result, EIS has emerged as an appropriate technique for labeled-free detection. Moreover, the EIS technique can be used as a clinical diagnostic tool for detecting cancer cells that are circulating in the patient's body using a non-invasive and cost-effective technique [51, 52, 53].

1.2.4 Materials

1.2.4.1 Polyaniline

Many conducting polymers have been applied in biosensor field, for example polyaniline (PANI), polyacetylene (PA), polythiophene (PT), poly(3,4-ethylenedioxythiophene) (PEDOT), polypyrrole (PPy), polyphenylene, and poly (phenylene vinylene). These conducting polymers can be synthesized with simple, versatile materials, and are cost-effective [54]. Polyaniline is a conductive polymer that is widely used among other conducting polymers [55]. Polyaniline is commonly used to modify the substrate of a working electrode because it contains an amine group, which facilitates biorecognition on the electrode surface [56]. In addition, the conductive property is used to improve sensor sensitivity [57]. Polyaniline has the advantages such as being simple to synthesize, good environmental stability, and highly conductive material in the doping state [58]. During the polymerization process of aniline monomer, polyaniline typically

exhibits three different oxidation states: leucoemeraldine (totally oxidized polyaniline), emeraldine (half oxidized or reduced polyaniline), and pernigraniline (fully reduced polyaniline). Especially, emeraldine can be formed into two states, including emeraldine base and emeraldine salt. Among the polyaniline forms, only emeraldine salt is in the conductive state, but it is conductive in acidic solutions with a pH of less than 3. When the polyaniline is treated in a solution with a pH greater than 3, it transforms into an insulator [54]. Moreover, the polyaniline structures of each oxidation state appear imine (=N-) and amine (-NH-) groups on the surface, making them suitable for surface modification [59].

The formation of polyaniline on electrode surface is carried out via electropolymerization process. The electrosynthesis is an extremely effective technique for synthesizing conductive polymer. The method of electrodeposition is separated into two categories. Firstly, anodic electrochemical polymerization is most commonly used to prepare conducting polymers by forming an oxidative monomer radical cation. Secondly, cathodic electrochemical polymerization is rarely used for the synthesis of conducting polymers because it involves reductive processes of monomers that result in a very low yield of conducting polymers [60]. During the electropolymerization of aniline monomer, emeraldine salt is formed to conductive polyaniline in the reduction state that is followed by four steps: including 1) oxidation of aniline monomer, 2) formation of dimers through the coupling of monomer cation radicals, 3) polymeric chain is grown from oxidation of dimers, then further reaction of dimers with monomer cation radicals, and 4) the polymeric chain is spontaneously doped for forming conducting polymer [61].

1.2.4.2 Gold nanoparticles based electrochemical immunosensors

Gold nanoparticles (AuNPs) are tiny gold particles with diameters ranging from 1 to 100 nm [62]. They are popular metal nanomaterials that are commonly used due to their unique properties such as a high surface area to volume ratio, material biocompatibility, improving the conductivity of electrode surface, and electron transfer facility to electrode surface [63]. The effect of AuNPs in electrochemical immunosensors is to improve the electrochemical signal, resulting in increased sensitivity for detecting various analytes. AuNPs act as a bridge between the redox protein and the bulk electrode surface, facilitating direct electron transfer. They can increase the amount of antibody immobilization [63]. In addition, AuNPs also are used to increase the density of redox peaks in various types of electrodes for immunosensor development. There are three

methods for electrode surface modification with gold nanoparticles: (1) self-assembled monolayers (SAMs) formed by using functional groups for binding gold nanoparticles, (2) electrochemical deposition of gold nanoparticles onto an electrode surface, and (3) mixing of gold nanoparticles with other components for formation on an electrode surface [64, 65].

1.2.4.3 Streptavidin-biotin interaction

The techniques used to immobilize biorecognition on electrode surfaces include adsorption, covalent linker, entrapment, encapsulation, and affinity of biotin-protein interaction. One of the strong interactions that contains multiple hydrogen bonds and van der Waals is the one between protein and biotin [66, 67]. This strength is roughly ten times that of the antibody-antigen interaction [68]. There are three types of proteins that interact with biotin, namely avidin, streptavidin, and neutravidin. Streptavidin is the most suitable to use for interaction with biotin due to more specific than others, and low degree of nonspecific adsorption [69]. The biotin-streptavidin interaction is one of the most popular that is used for conjugation with biomolecule such as protein, lipids, nucleic acids, and antibodies. Streptavidin is derived from the bacterium *Streptomyces avidinii*, which contains a homotetramer capable of binding four biotin molecules. Streptavidin-biotin interaction has been used for the development of electrochemical immunosensors for several reasons, including 1) the streptavidin lacks carbohydrates that can bind non-specific such as lectin in normal tissue, 2) the streptavidin's isoelectric point (pI) is near neutrality, resulting in low electrostatic binding with non-specific, 3) the streptavidin is small in size, and 4) biotin molecules allow to bind macromolecules (such as antibody) without disturb their functions [70], and 5) the interaction between streptavidin and biotin is not only highly stable, but it also improves the ability of biotin-labeled antibodies to capture antigen via lock and key formation [68]. Additionally, streptavidin has a high protein thermostability that protects it from extreme pH solutions, high temperatures, reagent denaturation, and enzyme degradation. These characteristics are important for a wide range of immunosensor detection [71, 72]. Streptavidin can capture biotin-labeled biomolecules on sensor surfaces in 25 minutes at 37 °C, significantly reducing the time required for sensor modification [73].

1.2.4.4 Epithelial cell adhesion molecule (EpCAM)

Epithelial cell adhesion molecule (EpCAM, also known as CD326) is a 40 kDa transmembrane glycoprotein that has high expression in carcinomas. It is imperative for proliferation, metastasis, and invasiveness of tumor cells [74, 75]. EpCAM can form as an enemy to E-cadherin by disrupting of alpha-catenin or F-actin link that leads to loosening solid cell-cell adhesions [76]. EpCAM is low expression in normal epithelial tissue but overexpression in epithelial cancers, including breast cancer, colonic cancer and others [77]. The expression of EpCAM protein on the cancer cell surface can indicate the existence of epithelial cancer cells in cancer patients, therefore it has gained attention as a potential target for cancer therapy and detection [78]. Anti-EpCAM monoclonal antibody (EpCAM antibody) is a biorecognition that is very highly specific with EpCAM marker on epithelial cancer surface. It is an approach for detecting epithelial cancer cells with high efficiency. Many researchers used EpCAM antibodies for diagnosing epithelial cancer such as CellSearch, microfluidic systems and immunomagnetic technology [79, 80, 81]. It could be confirmed that the EpCAM antibody is one of the popular antibodies that can detect epithelial carcinomas with promising results.

1.2.5 Analytical performance

1.2.5.1 Linearity

Linearity is the ability of the condition method that acquires from proportional test results to the target analyte concentration [82]. The linearity is tested by measuring a series of target analyte concentrations in at least three replications and plotting the relationship between signal response and the target analyte concentration. The correlation coefficient is commonly used to evaluate the method (r-value). When the correlation coefficient is close to one (0.9-0.99), the linear range is accepted [83].

1.2.5.2 Sensitivity

The sensitivity is defined as the slope of the calibration curve, which plots the signal response against the target analyte concentration. Sensitivity offers a change in analyte concentration leading to a change in signal measurement [84]. When a small change in target analyte concentration causes a large change in signal response measurement, this is referred to as high sensitivity [85]. The slope of the relationship between the response of charge transfer

resistance (ΔR_{ct}) and the analyte concentrations were used to determine the sensitivity of immunosensor fabrication in this work.

1.2.5.3 Limit of detection

In an electrochemical biosensor, the lowest concentration of an analyte that can be detected by the method is important to report. The limit of detection (LOD) value is used in reporting the minimum concentration of target analyte that can be reliably distinguished by the method. Several statistical methods including the signal-to-noise method, blank determination, and linear calibration curve can be used to calculate LOD [86].

1.2.5.4 Selectivity

The concentration of analytes is not directly measured. It quantifies based on a specific property (e.g., electrical signal conversion). However, the occurrence of a specific property is caused not only by the analyte but also by interference. Interference can cause the signal measurement to increase or decrease, resulting in a bias in the result [87]. The selectivity is determined by precisely measuring the analyte of interest in a sample solution containing various interference under conditions similar to those found in real sample solutions [82]. The selectivity of the immunosensor was estimated in this study based on the response of EpCAM antibody to EpCAM antigen biomarker on cancer cell surface by considering possible cancer cell types found in human blood. They are including MCF-7 cells (overexpressed EpCAM antigen) [88], A2780 cells (lower expressed EpCAM antigen) [89], and MG63 cell (non-expressed EpCAM antigen) [90].

1.2.4.5 Reproducibility

Reproducibility is the ability of a conditioning method to produce the same result when repeated under similar conditions. The precision and accuracy of the method are referred to as reproducibility. Precision means that the method can produce the same results every time an analyte is measured, whereas accuracy means that the method can produce results that are close to the true value if an analyte is measured more than once [91]. The reproducibility was calculated using experimental data and expressed as a percentage of relative standard deviation (percent RSD), indicating the acceptability of the immunosensor development [84]. The reproducibility of this thesis was calculated by comparing the analyte response to each electrode in the same condition and instrument in the same environment.

1.3 Objective

The purpose of this thesis is to develop an electrochemical immunosensor based on polyaniline and gold nanoparticles for CTCs detection using a screen-printed gold electrode

1.4 Outline of the research

This work focused on developing the electrochemical immunosensor based on polyaniline and gold nanoparticles using a screen-printed gold electrode (SPAuE) with good performance for CTCs detection. the immunosensor was fabricated by direct electropolymerization of aniline as the first layer on SPAuE for creating amine group on the surface for binding with streptavidin protein through EDC/NHS after electrodepositing gold nanoparticle as material that improves the electrochemical signal. In the process of immobilization probe, a biotin-EpCAM antibody was performed by using streptavidin-biotin interaction. The experimental section was proved through a microscope image, FE-SEM image, and an electrochemical technique. Finally, the analytical performances of developed immunosensor

CHAPTER 2

MATERIALS AND METHODS

2.1 Reagents

2.1.1 Electrode modification

- Aniline monomer (ANI, 99%, Sigma-Aldrich)
- Perchloric acid (HClO_4 , 69-72%, Merck)
- Tetra chloroauric (III) acid trihydrate ($\text{HAuCl}_4 \cdot 3\text{H}_2\text{O}$, Acros Organics)
- Sulfuric acid (H_2SO_4 , 98%, Sigma-Aldrich)
- N-(3-Dimethylaminopropyl)-N'-ethylcarbodiimide hydrochloride (EDC, Merck)
- N-Hydroxysuccinimide (NHS, Sigma-Aldrich)
- Streptavidin from *streptomyces avidinii* (SA, essentially salt-free, lyophilized powder, > 13 units/mg protein, Sigma-Aldrich)
- Biotin anti-human CD 326 (EpCAM) antibody (Clone: CO17-1A, BioLegend[®])
- Bovine Serum Albumin (BSA, lyophilized powder, $\geq 96\%$, Merck)
- Sodium dihydrogen phosphate monohydrate ($\text{NaH}_2\text{PO}_4 \cdot \text{H}_2\text{O}$, Merck)
- Di-sodium hydrogen phosphate dihydrate ($\text{Na}_2\text{HPO}_4 \cdot 2\text{H}_2\text{O}$, Merck)
- Potassium hexacyanoferrate (II) trihydrate ($\text{K}_4\text{Fe}(\text{CN})_6 \cdot 3\text{H}_2\text{O}$, Sigma-Aldrich)
- Potassium hexacyanoferrate (III) ($\text{K}_3\text{Fe}(\text{CN})_6$, Sigma-Aldrich)
- All aqueous solution was completed using water purified with a Milli-Q purification system (resistivity $\geq 18 \text{ M}\Omega \text{ cm}$)

2.1.2 Cell culture experiment

- Phosphate buffer saline pH 7.0 (PBS, HIMEDIA[®])
- Dulbecco's Modified Eagle Medium (1X) (DMEM, Gibco, UK)
- Fetal Bovine Serum (FBS, Gibco, Germany)
- GlutaMAX[™]-I (100X) (Gibco, Japan)
- Penicillin Streptomycin (Gibco, USA)
- Trypsin-EDTA (1X) (0.25%, Gibco, Canada)
- Lipophilic Carbocyanine Dyes (DiD, Molecular probes, USA)

2.2 Apparatus

- Potentiostat/ galvanostat Autolab, monitored by the NOVA 2.1.4 software (Metrohm, Netherland)
- Screen-printed gold electrodes (SPAuEs) (DropSens, Metrohm, Netherland)
- Field Emission Scanning Electron Microscope (FE-SEM, quanta 400, FEI company, Czech Republic)
- Lionheart FX Automated Microscope (Agilent, USA)

2.3 Immunosensor fabrication

The pretreatment of a SPAuE was carried out in 0.50 mol/L H₂SO₄ by using cyclic voltammetry (CV). Then, applying potential from 0 to 1.10 V with 100 mVs⁻¹ scan rate for 10 cycles was performed, followed by rinsing with ultrapure water and blowing with nitrogen gas. Before the working electrode surface was modified with polyaniline (PANI), its surface was gently washed with 50 mmol/L HClO₄ to adjust the surface to be the same as aniline solution. Subsequently, the electropolymerization process of aniline was operated in 4.0 mmol/L aniline (in 50 mmol/L HClO₄) via CV method in the potential range of -0.40 to +0.80 V at a scan rate of 50 mV s⁻¹ for 10 cycles [92]. The PANI-modified SPAuE (PANI/SPAuE) was washed with 50 mmol/L HClO₄ to remove the fragment of aniline. In addition, PANI-modified SPAuE was slightly washed with 0.50 mol/L H₂SO₄ to adjust the electrode surface similar to HAuCl₄·3H₂O solution. The electrodeposition of gold nanoparticles (AuNPs) was performed on the PANI/SPAuE in 0.60 mmol/L HAuCl₄·3H₂O (in 0.50 mol/L H₂SO₄) solution via CV by using a potential range

from -0.20 V to +1.2 V at a scan rate of 100 mV s^{-1} for 15 cycles [92]. Then, AuNPs-modified on PANI/ SPAuE (AuNPs/PANI/SPAuE) was washed with ultrapure water to remove residual $\text{HAuCl}_4 \cdot 3\text{H}_2\text{O}$ and dry with nitrogen gas.

For EpCAM immobilization, 50 μL of 1 mg/mL streptavidin was activated in 1 mL of EDC/NHS (100 mmol/L /200 mmol/L) for 30 minutes at 25 °C. Next, the activated streptavidin (10 μL) was placed on the surface of AuNPs/PANI/SPAuE and incubated for 2 hours at room temperature in a petri dish wrapped with parafilm. After incubation, the streptavidin-modified SPAuE (SA/AuNPs/PANI/SPAuE) was gently washed with 200 μL ultrapure water to remove the unbound activated streptavidin, and followed by blowing nitrogen gas. In the next step, 4 μL of 100 $\mu\text{g}/\text{mL}$ biotin-EpCAM antibody (in 10 mmol/L phosphate buffer, pH 7.4) was added on the streptavidin-modified SPAuE surface and incubated for 1 hour at 25 °C in a petri dish wrapped with parafilm. After that, the biotin-EpCAM modified SPAuE (b -EpCAM/SA/AuNPs/PANI/SPAuE) was washed with 200 μL of 10 mmol/L phosphate buffer (pH 7.4) to remove the unbound biotin-EpCAM and gently blown with nitrogen gas. Finally, to block the non-specific binding on the b-EpCAM/SA/AuNPs/PANI/SPAuE, 4 μL of 1% BSA was coated onto the modified SPAuE surface and incubated further for 30 minutes and followed by gently washing with 200 μL of 10 mmol/L phosphate buffer (pH 7.4). The modified SPAuE was finally stored at 4 °C before use.

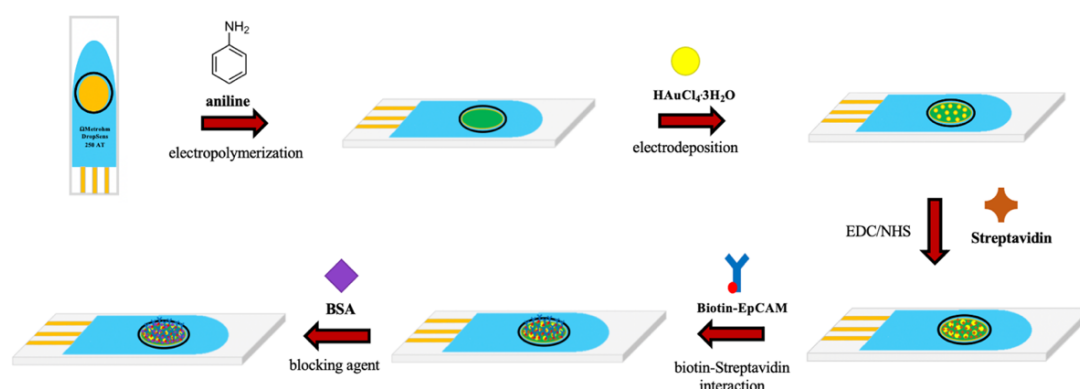


Figure 2.1 Schematic presentation of the process of the developed immunosensor using a SPAuE

2.4 Cell-culture experiment

MCF-7 cells were treated in a DMEM complete medium that consists of 10% FBS, 1% GlutaMAX (100X), and 1% Penicillin Streptomycin. The MCF7 cells were then kept in an incubator at 37 °C containing 5% CO₂. MCF-7 cells were monitored on a daily culture to ensure the medium without contamination and evaporated until obtaining 70-80% confluence of MFC-7 cells. To prepare MCF-7 cells for testing, the MCF-7 DMEM medium was removed and cleaned residual DMEM with 1X PBS. Then, the MCF-7 cells were trypsinized using 0.25% Trypsin-EDTA and incubated at 37 °C for 2-3 minutes. Subsequently, DMEM complete medium was added for blocking the activity of trypsinization. After that, MCF-7 cells were resuspended by gentle pipetting up and down. Finally, cell suspensions were prepared in 1XPBS before using as a sample for CTCs detection.

2.5 MCF-7 cell dyeing

Carbocyanine dye or DiD was added in 1X PBS solution pH 7.2 (final concentration 1 μM) that contains MCF-7 cells for labeling cytoplasmic and intracellular membrane structures. Then, it was mixed well and incubated in the MCF-7 cell at 37 °C containing 5% CO₂ atmosphere for 10 minutes. After that, MCF-7 cells were washed by removing the staining solution and adding 1X PBS pH 7.2 solution 3 times. Finally, MCF-7 cell staining was prepared in 1X PBS pH 7.2 before investigating with a fluorescence microscope.

2.6 Fluorescence microscope detection

MCF-7 cell staining at a concentration of 10,000 cells/mL was added to the developed immunosensor and stored at 37 °C with a 5% CO₂ atmosphere for 30 minutes. Then, the MCF-7 cell on the developed immunosensor was covered with a cover slip and investigated with Lionheart FX Automated Microscope in a fluorescent field in the dark mode and bright field by using outsource light.

2.7 Electrochemical measurement

Before MCF-7 cell detection, the developed immunosensor was pre-conditioned via CV. techniques. The CV was performed in 10 mL of 10 mmol/L phosphate buffer (pH 7.4) by applying the potential range from +0.20 V to +0.90 V at a scan rate of 100 mVs⁻¹ for 10 cycles. The different concentrations of MCF-7 cells were prepared in 1X Phosphate buffer saline (PBS) pH 7.2, including 10¹, 10², 10³, 10⁴, 10⁵ and 10⁶ cells/mL. Then, 5 µL of each MCF-7 concentration was dropped on the developed immunosensor and stored at 37 °C containing 5% CO₂ atmosphere for 30 minutes. Before electrochemical measurement was performed, the immunosensor was gently washed by dipping up and down in 1X PBS three times to remove non-specific and unbound MCF-7 cells. To evaluate the performance of the developed immunosensor, the different concentrations of MCF-7 cells were detected in 10 mM [Fe(CN)₆]^{3-/4-} containing solution of 10 mmol/L phosphate buffer (pH 7.0) [93] via EIS technique in the frequency range from 10⁵ to 10⁻¹ Hz, and signal amplitude of 5 mV at 5 points per decade.

2.8 Linear range

The developed immunosensor was examined at various concentrations of MCF-7 cells from low to high concentration in solution of the redox mediator. The change of charge transfer resistance was related to the amount of MCF-7 cells which were captured on the developed immunosensor. A calibration curve was plotted between the increase of charge transfer resistance (ΔR_{ct}) and MCF-7 cell concentrations.

2.9 Limit of detection

The limit of detection (LOD) is used to explain the lowest quantity or concentration of MCF-7 cells that can be measured reliably and with statistical significance. It was an estimate based on linear regression by the following equation [86].

$$\text{LOD} = \frac{3\text{SD}}{S} \quad (1)$$

Where SD is the standard deviation of the reflection computed by the standard deviation of y-intercepts in regression lines, and S is the sensitivity (sloop) of the calibration curve.

2.10 Selectivity

The selectivity of the modified SPAuE was examined at the same concentration under the modified condition. This performance was studied with three different types of cancer cells including MCF-7 cell as over-expressed EpCAM antigen, A2780 cell as low-expressed EpCAM antigen, and MG-63 as non-expressed EpCAM antigen. These cancer cells were prepared in 1X PBS (pH 7.2), and also 1X PBS pH 7.2 was used as a control in this testing. For the testing, the concentration of different cancer cells was used at 1,000 cells/mL and 100,000 cells/mL for observing R_{ct} response to different types of cancer cells. Additionally, the three types of cancer cells were mixed well and tested at the same condition. The testing was evaluated through the EIS technique at the frequency range from 10^5 to 10^{-1} Hz and signal amplitude of 5.0 mV at 5 points per decade.

2.11 Reproducibility

Five SPAuEs were modified under the same method above in a section of the modified sensor, and used for testing 100 cells/mL MCF-7 cell in a solution of 10 mM $[\text{Fe}(\text{CN})_6]^{3-/4-}$ containing 10 mM phosphate buffer, pH 7.0. The EIS technique was performed at a frequency range from 10^5 to 10^{-1} Hz and signal amplitude of 5.0 mV at 5 points per decade. The results of ΔR_{ct} response of each modified SPAuEs to MCF-7 cell were investigated. The acceptability of this fabricated immunosensor was evaluated by calculating the % relative standard deviation (%RSD) of the ΔR_{ct} response of each modified SPAuE under similar the modified sensor method and environment (at 25 °C).

CHAPTER 3

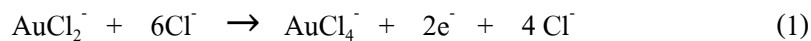
RESULTS AND DISCUSSION

3.1 Immunosensor fabrication

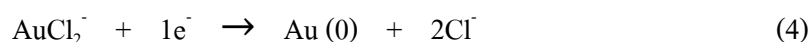
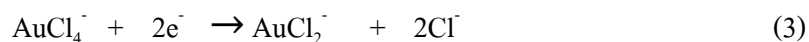
3.1.1 Surface characterization of the AuNPs/PANI-modified electrodes

The surface morphologies of the modified SPAuE were investigated using a field emission scanning electron microscope (FE-SEM) to confirm the success of polyaniline and AuNPs formation. Following the condition of aniline electropolymerization [92], PANI structure formed on the SPAuE surface after the oxidation reaction of aniline monomer in the potential range of 0.2 to 0.4 V. As shown in Figure 3.1A, the cyclic voltammograms of aniline showed an increase in the anodic peaks (oxidation reaction) which indicates aniline monomer being formed to polyaniline structure on SPAuE surface [94]. The formation of PANI through electropolymerization was followed by four procedures. The first was the oxidation of aniline monomer (formation of monomer cation-radical). The second was the formation of dimers through a coupling of monomer cation radicals (by deprotonation and re-aromatization). The third, polymeric chain was grown through the oxidation of dimers and further reaction of dimers with monomer cation radicals. Finally, the polymeric chain was spontaneously doped to form conducting polymer [95]. The obtained FE-SEM image revealed that PANI formed a dense nanorod-like structure with an average diameter of 40 ± 14 nm (Figure 3.1B). However, the result of the PANI structure on the SPAuE surface was different from previous report [92] that they had reported as small particles. The difference in PANI structure depends on many factors such as monomer concentration, pH of medium, acidic doping, synthesis method, and electrode materials. Especially the difference in the surface of the electrode (SPAuE) that being chosen to form PANI in the previous study is importance for oxidation of aniline [96, 97]. Then AuNPs were electrodeposited on the PANI/ SPCE via cyclic voltammetry as shown in Figure 3.2A. It can be seen that the anodic peak a indicated that the gold oxidation to Au^{3+} as shown in equation (1) and peak b presented

the oxidation of chloride to chlorine as displayed in equation (2). Besides, the anodic peak c occurred due to oxygen evolution.



In addition, cathodic peak d is represented the reduction of Au^{3+} , as seen in equation (3), cathodic peak e is assigned to the reduction of Au^+ to AuNPs, as displayed in equation (4), and cathodic peak f is specified to hydrogen evolution [98, 99, 100]



The success of deposited AuNPs on the surface of the PANI layer was confirmed through SEM image (Figure 3.2B). The tiny beads were observed with an average diameter of 35 ± 10 nm and distributed well on the PANI surface, similar to that of the previous report [92]. Regarding differential pulse voltammograms (DPV) results (Figure 3.3), the appearance of PANI structure after electropolymerization was related to an increase in the oxidation peak current of $[\text{Fe}(\text{CN})_6]^{3-/4-}$ to 90 μA (trace b), while a bare SPAuE was responded to 60 μA (trace a). This is due to PANI material providing electrical conductivity, which can be observed at 0.05 V. The increase in current signal could confirm that the PANI modification on the SPAuE was successful. When AuNPs modification, the oxidation peak of $[\text{Fe}(\text{CN})_6]^{3-/4-}$ increased significantly to 115 μA (Figure 3.3, trace c) which is related to the appearance of a tiny bead of AuNPs. This is due to AuNPs provided high electroactive material, leading to the conductivity enhancement of the AuNPs/PANI/SPAuE. Thus, the increase in the current signal could provide strong evidence to confirm the presence of AuNPs on the PANI/SPAuE surface.

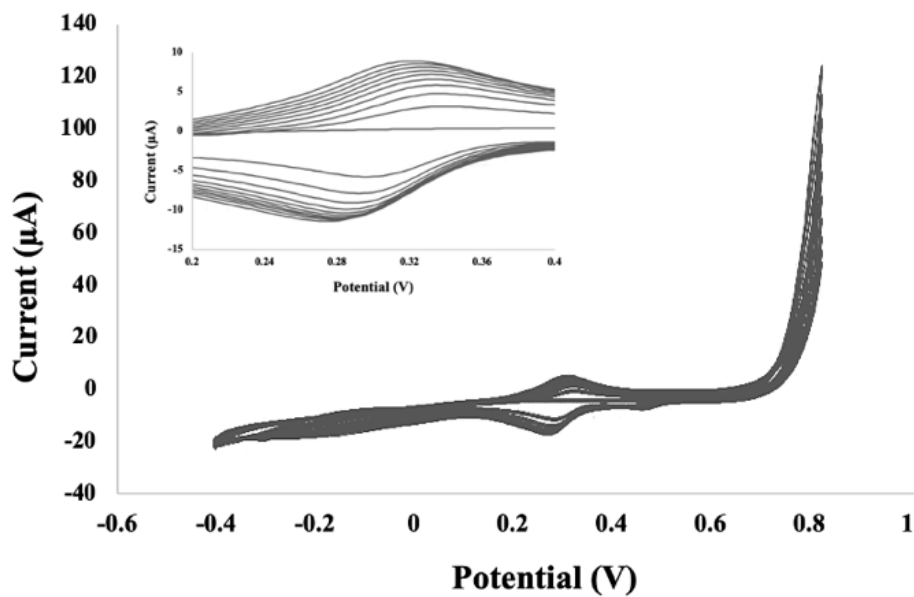
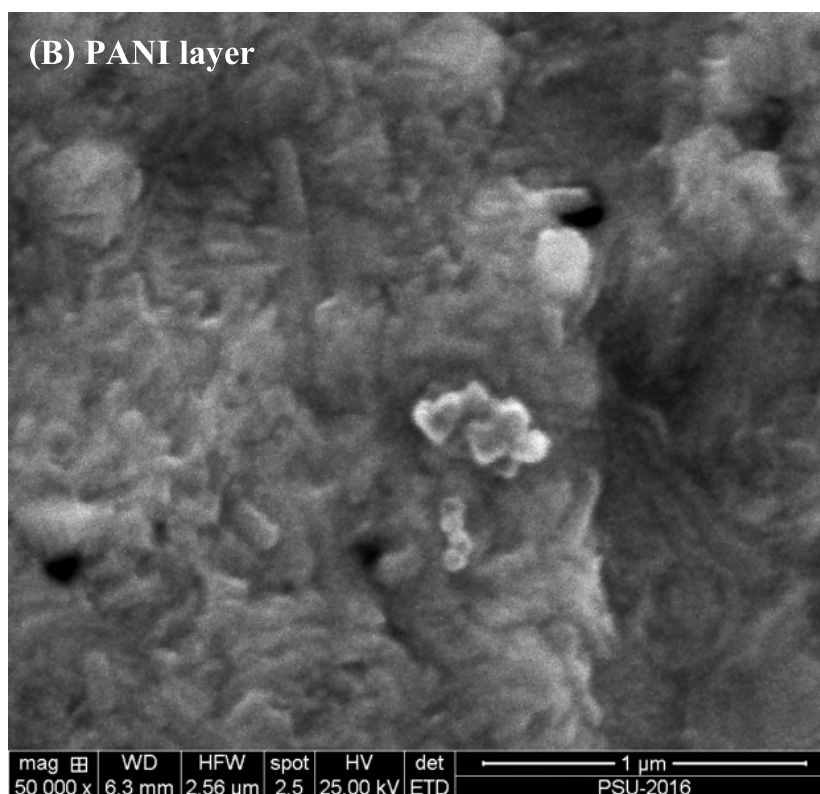
(A) Electropolymerization process**(B) PANI layer**

Figure 3.1 (A) electropolymerization process of aniline in 50 mM HClO₄ in the potential range of 0.2 to 0.4 V at a scan rate of 50 mV s⁻¹ for 10 cycles by CV technique and (B) FE-SEM image of the PANI forming layer prepared by 4 mM aniline monomer on SPAuE surface.

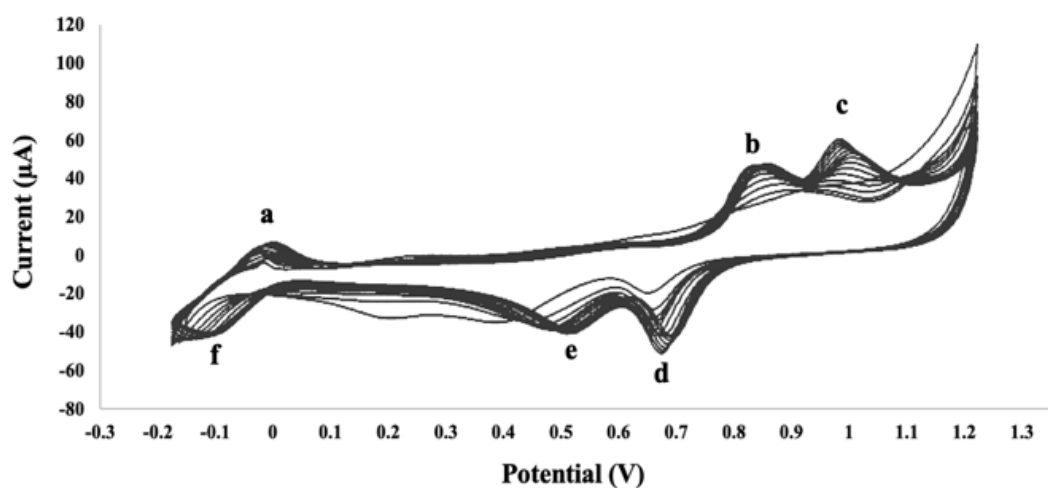
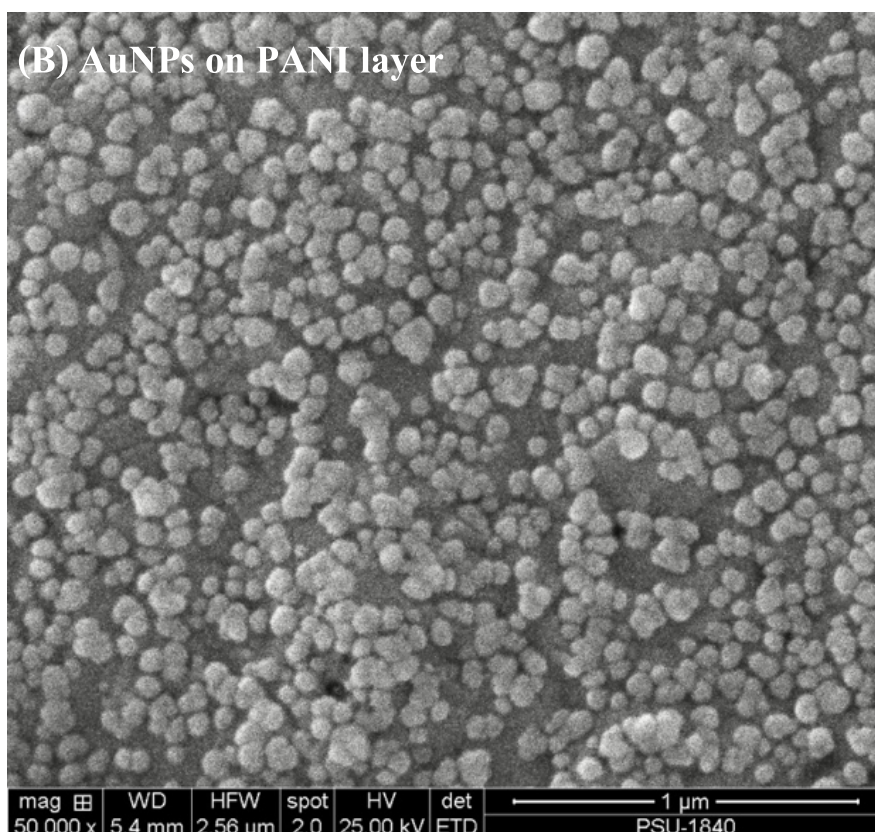
(A) Electrodeposition process**(B) AuNPs on PANI layer**

Figure 3.2 (A) the electrodeposition process with 15 cycle scans of 0.6 mM HAuCl_4 in 0.5 M H_2SO_4 to form AuNPs and (B) FE-SEM image of PANI modified SPAuE surface after AuNPs deposition.

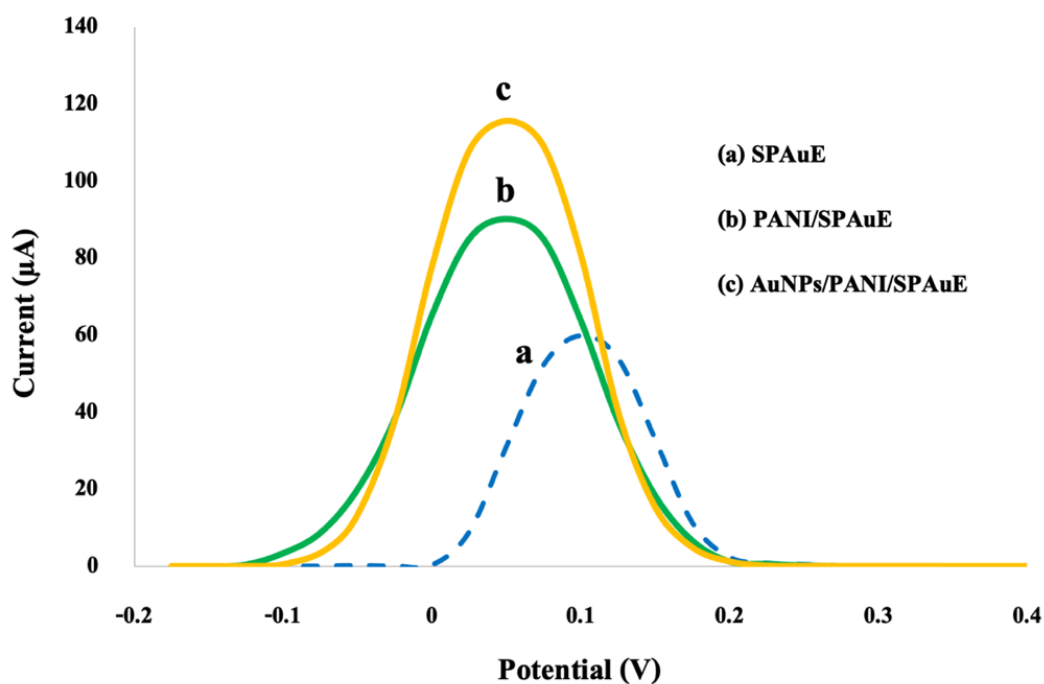


Figure 3.3 Differential pulse voltammograms (DPV) showing the current responses of (a) bare SPAuE, (b) PANI/SPAuE, and (c) AuNPs/PANI/SPAuE in 10 mM $[\text{Fe}(\text{CN})_6]^{3-/4-}$ containing 10 mM phosphate buffer at pH 7.0.

3.1.2 Electrochemical characterization of the developed immunosensor

The success of each modification step was also electrochemically characterized by electrochemical impedance spectroscopy (EIS). EIS technique is commonly used to confirm the presence of modified material on an electrode surface based on electron transfer resistance behavior. Figure 3.4 shows the EIS results which were obtained from charge transfer resistance detection and table 1 obtained from equivalent circuit fitting in each step of the immunosensor fabrication. At a bare SPAuE, the charge transfer resistance (R_{ct}) obtained from the diameter of the Nyquist plot semicircle was 821.21 Ω , which can be observed in the trace a. After electropolymerization of aniline on the bare SPAuE, R_{ct} of PANI/SPAuE clearly decreased to 88.35 Ω (trace b). The decrease of R_{ct} could indicate that PANI provides a fast electron transfer dynamic, and good electrochemical activity. When AuNPs were electrodeposited on the PANI layer, the result found that R_{ct} decreased to 55.7 Ω (trace c), due to AuNPs allowing an electron of redox solution to

transfer easily to SPAuE surface, causing R_{ct} decreased [9, 92]. Following this step, streptavidin (SA) was bound on AuNPs/PANI/SPAuE surface. The result showed that its R_{ct} decreased to 21.46 Ω (trace d). This might be because the support of both AuNPs and PANI coated SPAuE surface leads to enhancing electron transfer between the active center of streptavidin protein and SPAuE surface [101, 102]. After b-EpCAM antibodies were then immobilized on streptavidin modified electrode, the result found that R_{ct} increased to 230.38 Ω due to the insulating property of EpCAM antibody that obstructed electron transfer (trace e). Finally, R_{ct} also increased to 420.06 Ω after the remaining reactive free area was covered by BSA (trace f), owing to the surface being blocked and leading to inhibiting electron transfer. Therefore, metamorphosis of electrochemical characterization confirmed that the modification of each step on SPAuE surface was successful in developing an EpCAM-based immunosensor.

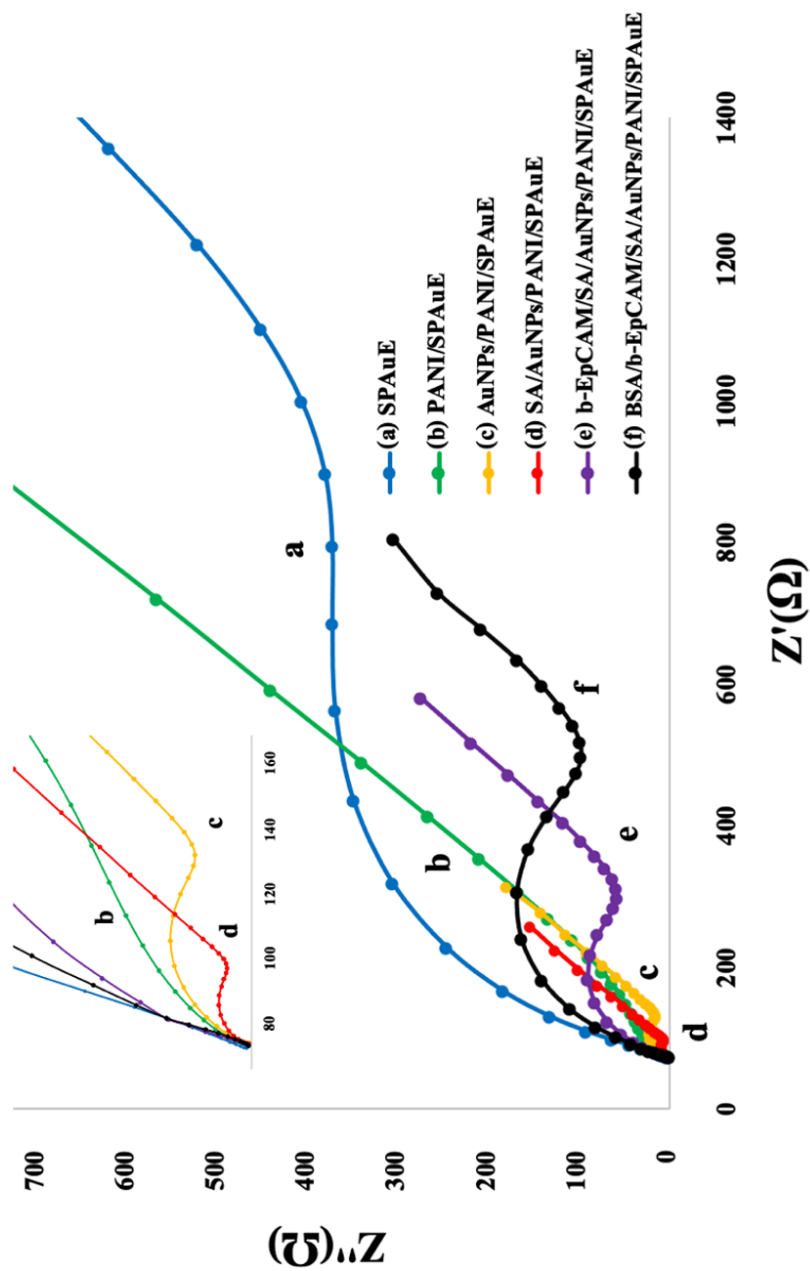


Figure 3.4 Nyquist plot of the developed SPAuE in each step was obtained in 10 mM $[\text{Fe}(\text{CN})_6]^{3-/4-}$ containing 10 mM phosphate buffer at pH 7.0 using EIS technique in the frequency range of 10^5 to 10^{-1} Hz with a signal amplitude of 5 mV (5 points per decade) at (a) bare SPAuE, (b) PANI/SPAuE, (c) AuNPs/PANI/SPAuE, (d) SA/AuNPs/PANI/SPAuE, (e) b-EpCAM/SA/AuNPs/PANI/SPAuE, and (f) BSA/b-EpCAM/SA/AuNPs/PANI/SPAuE.

Table 1 the data of SPAuE modification

A) The data of SPAuE

Element	Parameter	Value	Estimated Error(%)
Rs	R	73.637	0.778
Rp	R	821.210	2.076
CPE	Y_0	1.30×10^{-5}	5.497
	N	0.84123	0.897
W1	Y_0	0.004972	1.626
	X^2	0.012355	

B) The data of PANI/SPAuE

Element	Parameter	Value	Estimated Error(%)
Rs	R	71.511	5.437
Rp	R	88.348	2.982
CPE	Y_0	3.37×10^{-5}	9.223
	N	0.66712	8.203
W1	Y_0	0.004367	10.029
	X^2	0.010932	

C) The data of AuNPs/PANI/SPAuE

Element	Parameter	Value	Estimated Error(%)
Rs	R	73.549	0.326
Rp	R	55.700	1.933
CPE	Y_0	1.82×10^{-5}	11.181
	N	0.82707	2.41
W1	Y_0	0.005577	0.408
	X^2	0.009365	

D) The data of SA/AuNPs/PANI/SPAuE

Element	Parameter	Value	Estimated Error(%)
Rs	R	73.733	0.311
Rp	R	21.456	1.067
CPE	Y_0	3.00×10^{-5}	8.419
	N	0.78732	1.291
W1	Y_0	0.004835	0.531
	X^2	0.012355	

E) The data of b-EpCAM/SA/AuNPs/PANI/SPAuE

Element	Parameter	Value	Estimated Error(%)
Rs	R	69.385	0.581
Rp	R	230.38	1.165
CPE	Y_0	2.66×10^{-5}	6.179
	N	0.79186	1.044
W1	Y_0	0.004191	1.572
	X^2	0.010637	

f) The data of BSA/b-EpCAM/SA/AuNPs/PANI/SPAuE

Element	Parameter	Value	Estimated Error(%)
Rs	R	70.739	0.806
Rp	R	420.06	1.479
CPE	Y_0	2.31×10^{-5}	6.44
	N	0.81532	1.115
W1	Y_0	0.004874	3.073
	X^2	0.013539	

3.1.3 The effect of AuNPs on the streptavidin based immunosensor

The performances of streptavidin modified on PANI/SPAuE (SA/PANI/SPAuE) with and without AuNPs were studied by using CV and EIS techniques. As seen in Figure 3.5A, the EIS results showed that the R_{ct} of streptavidin modified PANI/SPAuE (SA/PANI/SPAuE) without AuNPs exhibited a significantly increase from 88 to 1000 Ω (Figure 3.5A, trace c) that was corresponding to decreasing in the current signal of CV (Figure 3.5B, trace c). This result was corresponding with the studies reported by [103, 104, 105]. Typically, it is noted that a protein molecule is an electrical insulator that enables to block the electron transfer between the redox solution and the electrode surface, leading to a decrease in the conductivity of the fabricated immunosensor. However, some molecules in protein such as amino groups can conduct when present on the electrode surface [106, 107], especially, coating on high conductive materials [101, 102].

In our study, when streptavidin was immobilized on the PANI/SPAuE with the presence of AuNPs, the R_{ct} of SA/AuNP/PANI/SPAuE decreased evidently from 55 to 20 Ω (Figure. 3.6A, trace d). The result was also confirmed by running CV as seen in Figure 3.6B. The CV result revealed, as shown in Figure 3.6B (trace d), that an increase in the CV current signal after SA immobilized AuNPs/PANI/SPAuE, being consistent with the EIS results. The CV results showed that the cathodic peak was shifted to the left because amino acid residues of streptavidin are active, leading to enhance the fast kinetics of the reaction [101, 108]., The increase in the conductivity of SA/AuNPs/PANI/SPAuE exhibited higher than the conductivity of SA/PANI/SPAuE. It could explain that an increase in the conductivity of the modified electrode occurred due to being induced by an influence of both PANI and AuNPs. It could be because AuNPs could induce amino acid residues (electroactive species) of streptavidin to facilitate electron transfer, enhancing the electron transfer between the active centre of streptavidin protein and SPAuE surface [101], and polyaniline as a solid mediator allowing electrons to shuttle [102]. However, a previous study found that streptavidin modified on gold nanoparticles without polyaniline exhibited non-conductivity [103]. This suggests that streptavidin was immobilized on both polyaniline and gold nanoparticles, resulting in high conductivity for the development of immunosensors.

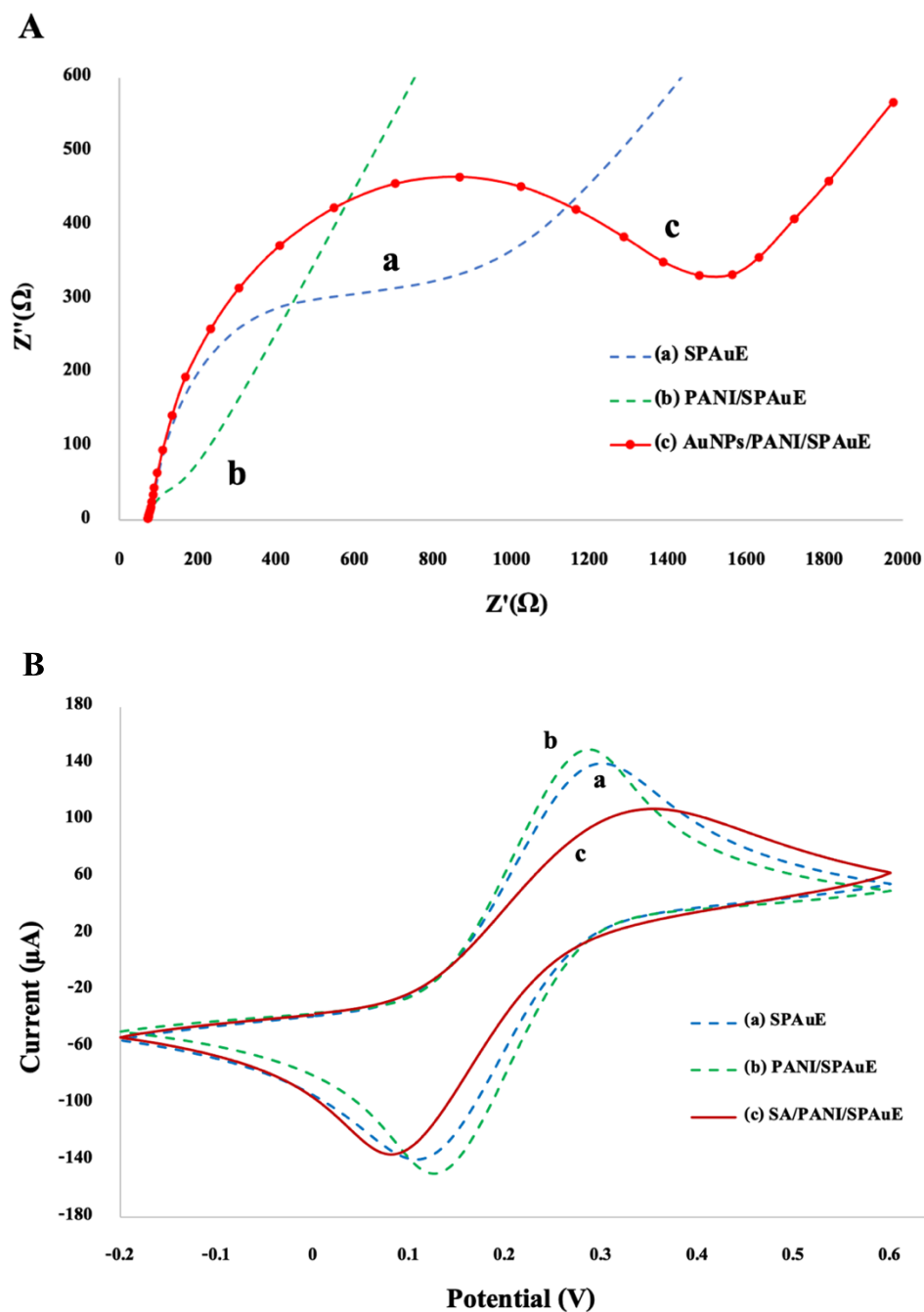


Figure 3.5 Streptavidin/polyaniline-modified SPAuE without AuNPs was detected with (A) EIS technique in the frequency range of 10^5 to 10^{-1} Hz with a signal amplitude of 5 mV (5 points per decade) and (B) CV technique in a potential range of -0.20 V to 0.60 V with a scan rate 50 mV s^{-1} . These processes were obtained in a 10 mM $[\text{Fe}(\text{CN})_6]^{3-/4-}$ containing 10 mM phosphate buffer at pH 7.0

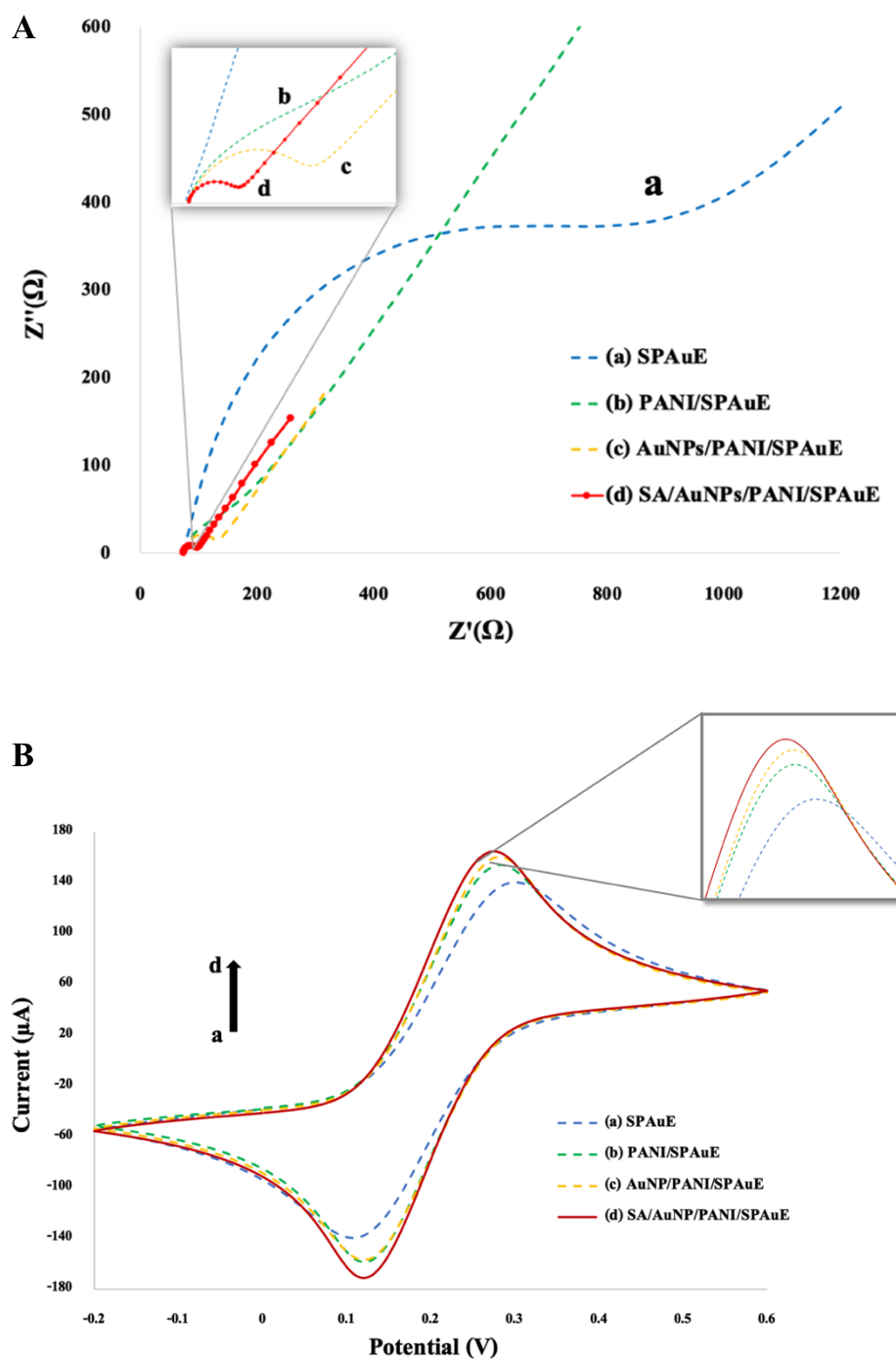


Figure 3.6 Streptavidin/AuNPs/polyaniline modified SPuE (the presence of AuNPs) was detected through (A) EIS technique in the frequency range of 10^5 to 10^{-1} Hz with a signal amplitude of 5 mV (5 points per decade) and (B) CV technique in a potential range of -0.20 V to 0.60 V with a scan rate 50 mV s^{-1} . These processes were obtained in 10 mM $[\text{Fe}(\text{CN})_6]^{3-/4-}$ containing 10 mM phosphate buffer at pH 7.0

3.2 Analytical performances of the developed immunosensor

Initially, the performance of the b-EpCAM/SA/AuNPs/PANI/SPAuE for capturing MCF-7 cells was examined by detecting 10,000 cells/mL of MCF-7 cells in 10 mM $[\text{Fe}(\text{CN})_6]^{3-/4-}$ containing 10 mM phosphate buffer (pH 7.0) via using EIS technique in a frequency range from 10^5 to 10^{-1} Hz and signal amplitude of 5 mV for 5 points per decade. As shown in Figure 3.7A, the EIS results revealed that the R_{ct} increased when MCF-7 cells were captured by EpCAM antibody on the modified SPAuE. This suggests that the MCF-7 cells were captured and prevented electron transfer, confirming the presence of 10,000 cells/mL of MCF-7 on the modified SPAuE. Fitting an equivalent electrical circuit model to the EIS results was used to analyze the results. It includes solution resistance (R_s), constant phase element (CPE) that substitutes double-layer capacitance due to capacitor non-ideality, charge transfer resistance (R_{ct}) of the modified SPAuE surface, and Warburg diffusion impedance (W) caused by the redox couple solution diffused from bulk solution to interface (Figure 3.7B). Abovementioned, the presence of MCF-7 cells on the modified SPAuE was confirmed based on differentiation of R_{ct} .

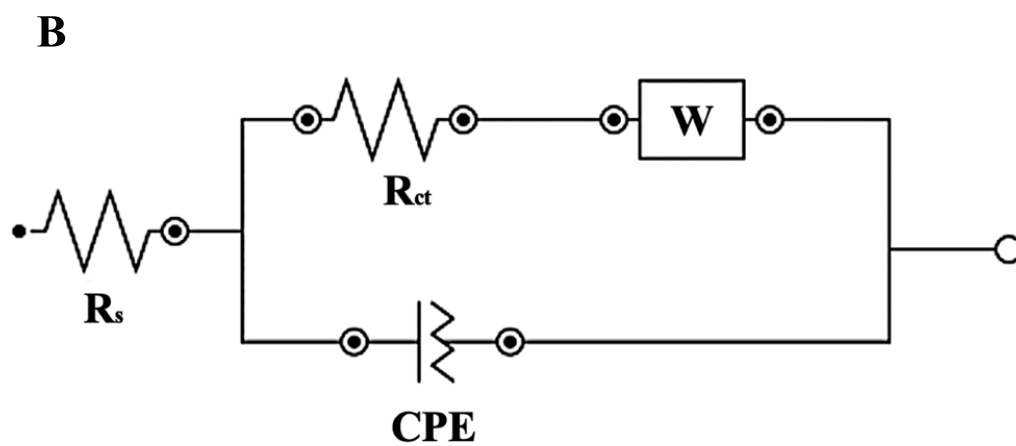
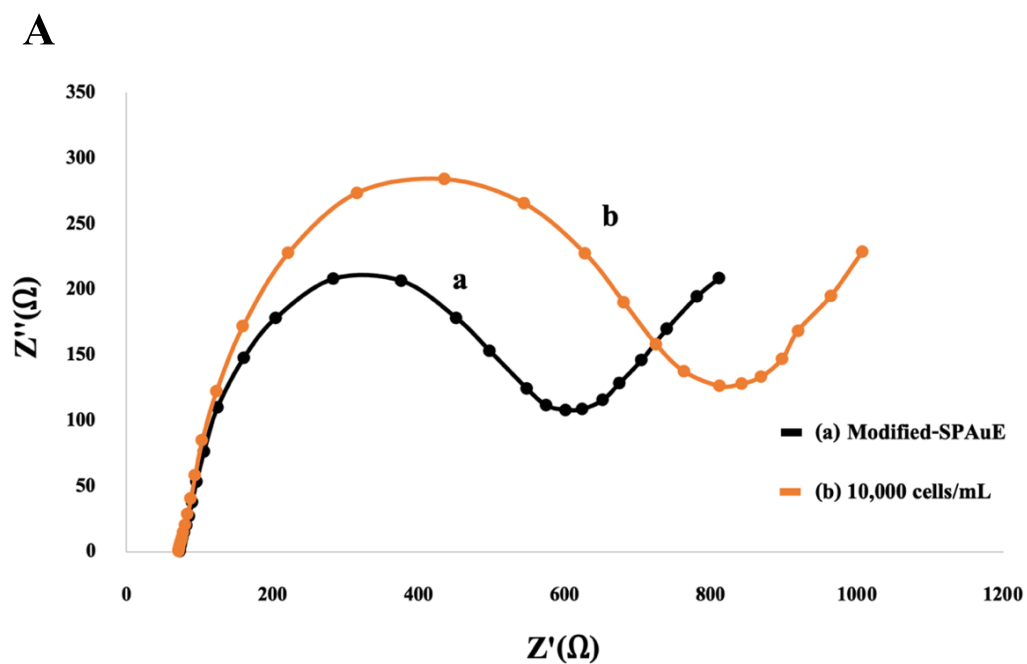


Figure 3.7 (A) EIS response before (trace a) and after (trace b) detecting 10,000 cells/mL of MCF-7 cells, and (B) Equivalent circuit for fitting the impedance spectra of Nyquist plot.

Furthermore, we also confirmed the presence of MCF-7 cells on the SPAuE using a fluorescence microscope by staining 10,000 cells/mL of MCF-7 cells with carbocyanine dye (DiD) to label cytoplasmic and intracellular membrane structures of MCF-7 cells and 1X PBS as control. The result showed that MCF-7 cells appeared on the modified SPAuE as a black dot in the bright field and an orange dot in the fluorescent field. When both images were merged, black and orange dots almost appeared in the same position as shown in Figure 3.8A. In the control group, any visible spots on the modified SPAuE surface, whether in the form of a bright field or a fluorescent field, are invisible (Figure 3.8B). The results indicated that our developed immunosensor was capable of capturing MCF-7 cells for detection.

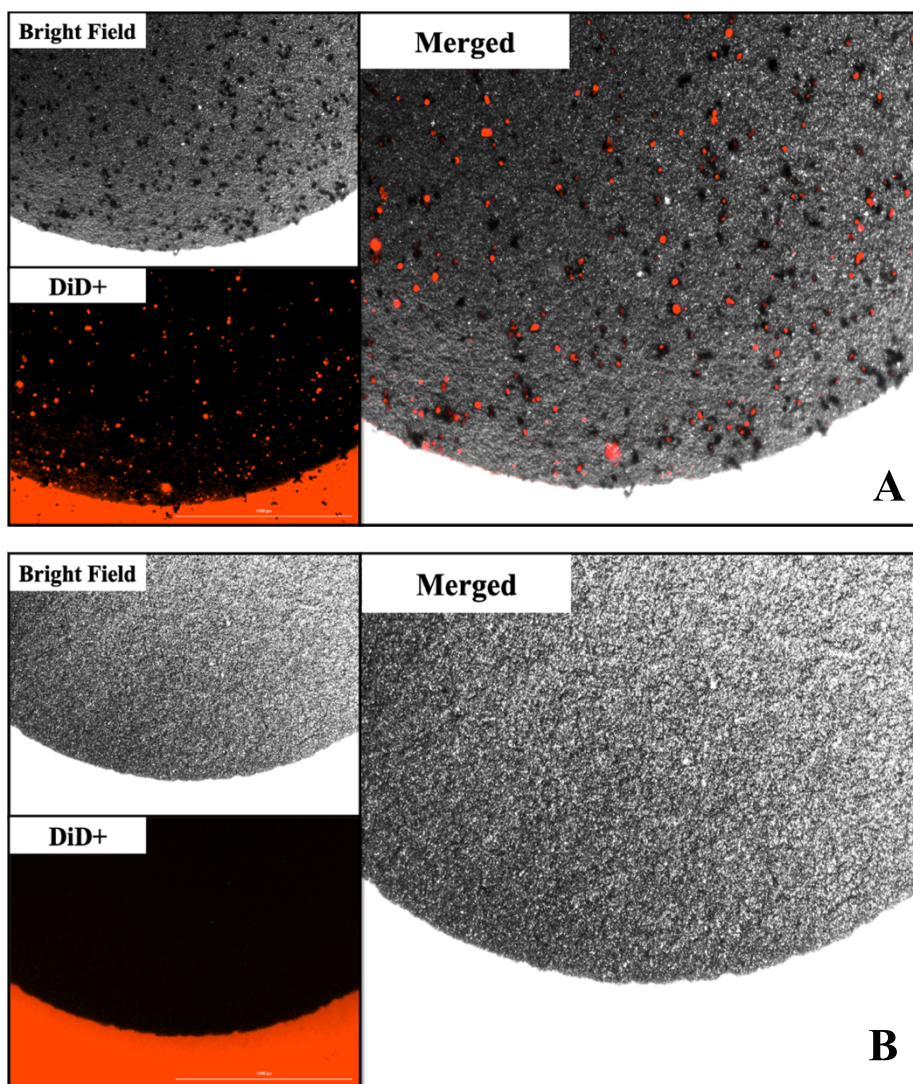


Figure 3.8 Microscope images of (A) the modified SPAuE with the presence of MCF-7 cells on surface and B) the modified SPAuE without MCF-7 cells on surface.

3.2.1 Linearity and limit of detection

The sensitivity of the immunosensor was determined through EIS response at various concentrations of MCF-7 cells. Figure 3.9 shows EIS spectra at the b-EpCAM/SA/AuNPs/PANI modified SPAuE after incubating MCF-7 cells for 30 minutes at different concentrations in a range from 10 to 10^6 cells/mL. It was found that the R_{ct} (the semicircle of EIS spectra) increased when MCF-7 cell concentrations increased. The calibration curve presented a linear relationship between the charge transfer resistance (R_{ct}) value and logarithm value of cumulative MCF-7 cell concentrations in the range of 10 to 10^5 cells/mL (Figure 3.10). The linear regression equation was $Y = 99.44 \log [C_{MCF-7}] + 52.085$, with a correlation coefficient of 0.9978. Additionally, when only 1 concentration at 1,000 cells/mL was tested with the developed immunosensor, we obtained R_{ct} around 226.78Ω ($n=3$) which is in the range of R_{ct} of 1,000 cells/mL. Therefore, the result of detection as series per an immunosensor or 1 sample concentration per an immunosensor is no different due to the number of MCF-7 cells that be used as a sample each time are average of 1,000 cells/mL.

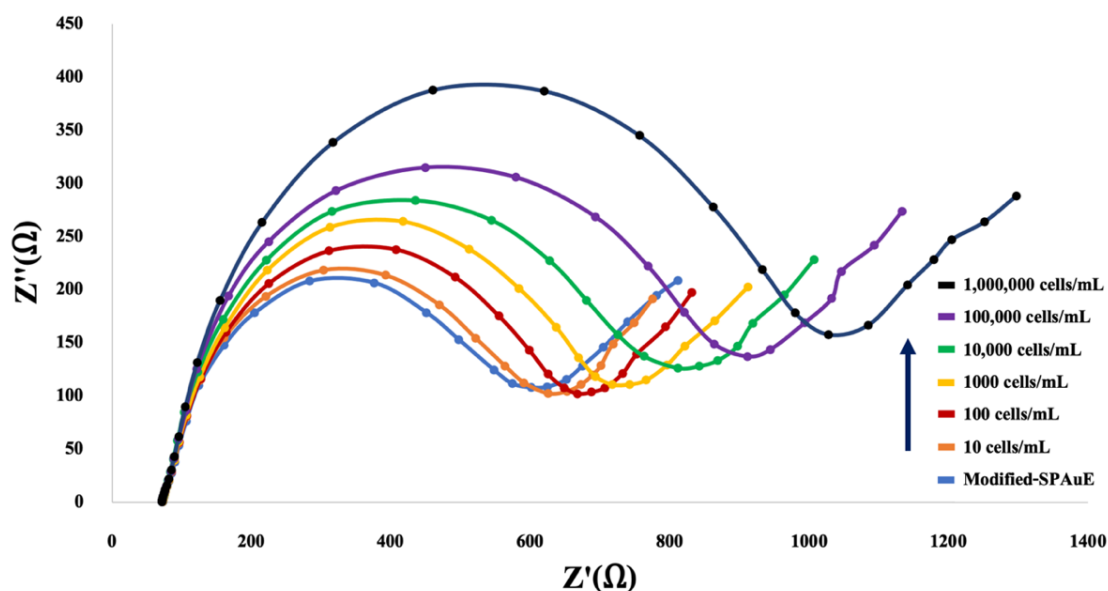


Figure 3.9 A cumulative graph illustration of EIS spectra response at various concentrations of MCF-7 cells in the range of 10 to 10^6 cells/mL. This process was achieved by detecting in the solution of 10 mM $[\text{Fe}(\text{CN})_6]^{3-/4-}$ containing 10 mM phosphate buffer pH 7.0

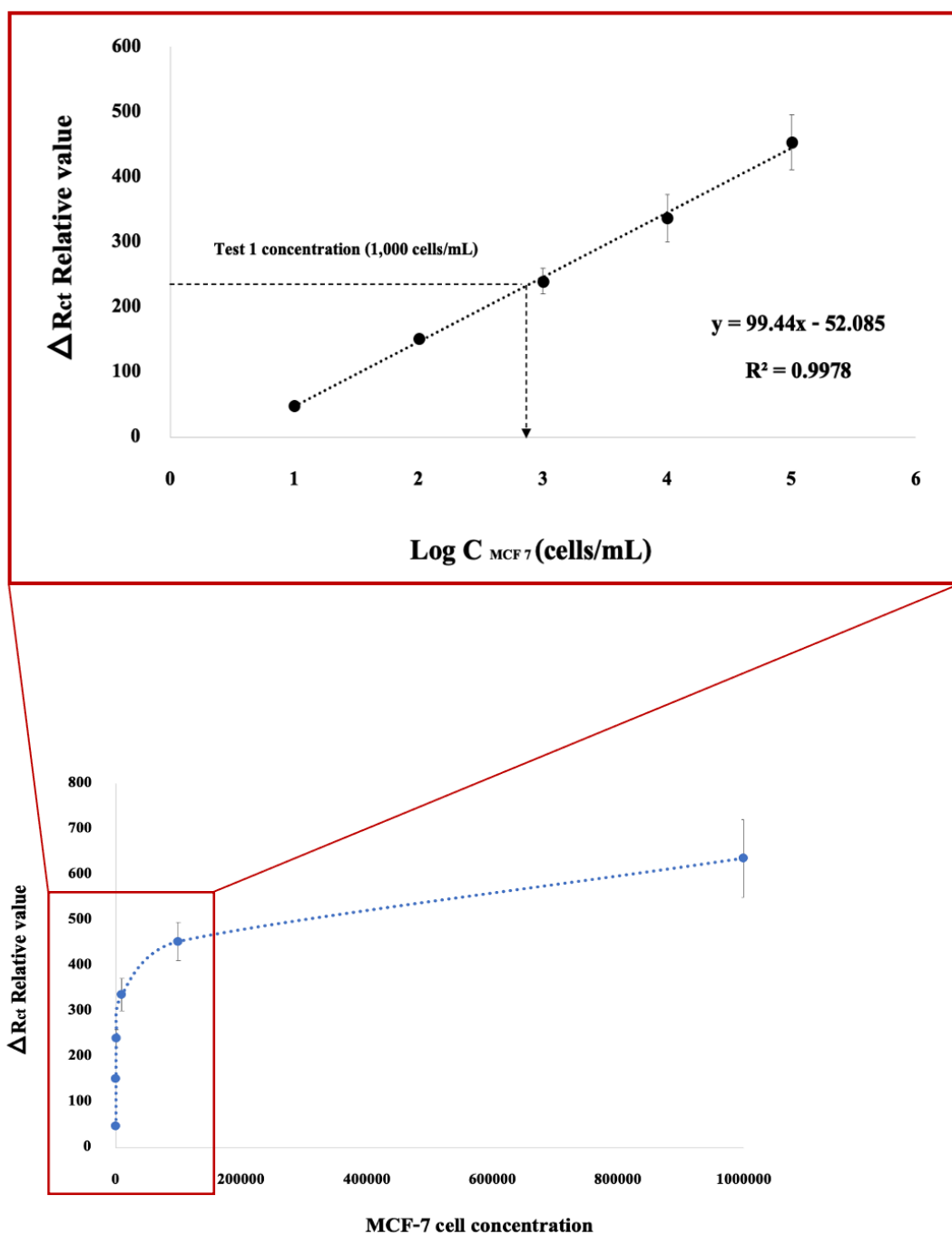


Figure 3.10 The calibration curve presented a linear relationship between the charge transfer resistance (R_{ct}) value and logarithm value of cumulative MCF-7 cell concentrations that adapt from the number of MCF-7 cell concentrations in the range of 10 to 10^5 cells/mL. The sensitivity was achieved by detecting in the solution of 10 mM $[\text{Fe}(\text{CN})_6]^{3-/4-}$ containing 10 mM phosphate buffer pH 7.0 (n=5)

The limit of detection (LOD) was determined at a signal-to-noise ratio of 3 (3S/N), where S is the standard deviation of the response (the standard deviation of y-intercepts) while N is the slope of the calibration curve. The LOD was found to be 2 cells/mL. Therefore, this developed immunosensor has a high potential to detect CTCs in low concentrations that were discovered in an early-stage cancer patient.

The principle of calculating the limit of detection

From formula ;

$$\begin{aligned} \text{LOD} &= 3S/N \\ &= 3(8.89)/99.44 \\ &= 0.268 \rightarrow X \end{aligned}$$

Due to

$$\log C_{\text{MCF-7}} = X$$

Then

$$C_{\text{MCF-7}} = 10^x$$

So

$$C_{\text{MCF-7}} = 10^{0.268}$$

$$\therefore \text{LOD} = 1.854 \approx 2 \text{ cells/mL}$$

3.2.2 Selectivity

The selectivity of the developed immunosensor was examined through the response of EpCAM antibodies to the epithelial cell adhesion molecule (EpCAM) antigens of MCF-7 cells, A2780 cells and MG 63 cells. Therefore, the expression of EpCAM antigen on cancer cell surface was used as a criterion to evaluate the specificity of this immunosensor in the same concentration and under conditions. As shown in Figure 3.11, the R_{ct} of MCF-7 cells was found to be the highest due to MCF-7 cell surface overexpression of EpCAM antigen, resulting in a large amount of captured MCF-7 cells on the modified SPAuE surface. As a result, electron transfer to the electrode surface was inhibited. While R_{ct} of A2780 cell had a lower signal response due to the low expression of EpCAM antigen, this resulted in a lower chance of A2780 cell capture. However, it should be noted that this phenomenon might occur owing to the expression of EpCAM antigen on the surface of each cancer cell. The R_{ct} of MG 63 cell was slightly higher than in the control (1X PBS). This is due to MG 63 cell nonspecific adsorption on the modified SPAuE surface.

Finally, the R_{ct} of cancer cell mixture (MCF-7 cells, A2780 cells, and MG 63 cells) was almost increased with the same along with an increasing proportion of A2780 cells and MCF-7 cells.

The result implied that the developed immunosensor was highly selective with the cancer cells that expressed EpCAM antigen on their surface. Especially, cancer cells were overexpression of EpCAMs as MCF-7 cells.

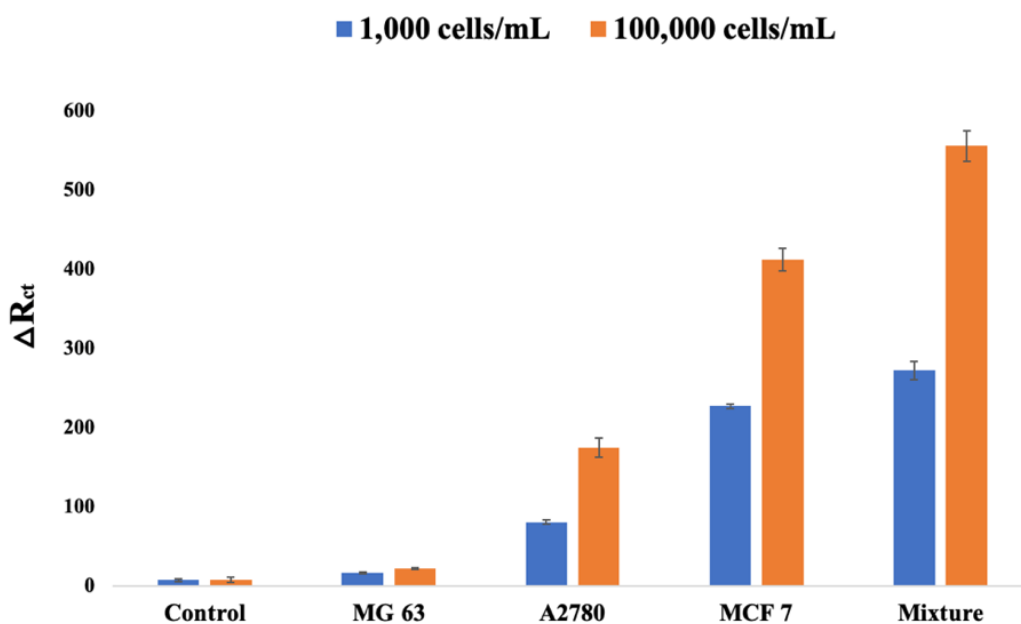


Figure 3.11 Effects of interfering on the response of the developed immunosensor to MCF-7, A2780, and MG 63 cells in 1X PBS solution at the concentration of 1,000 and 100,000 cells/mL of each type.

3.2.3 Reproducibility

The reproducibility was examined using five immunosensors. The five immunosensors were prepared in the same condition and tested with 100 cells/mL. As shown in Figure 3.12, the R_{ct} results were 149.00 Ω , 155.00 Ω , 145.00 Ω , 154.93 Ω , and 157.85 Ω , respectively. The result found that the five immunosensors obtained a relative standard deviation (RSD) of 3.43% for 100 cells/mL, indicating acceptable reproducibility.

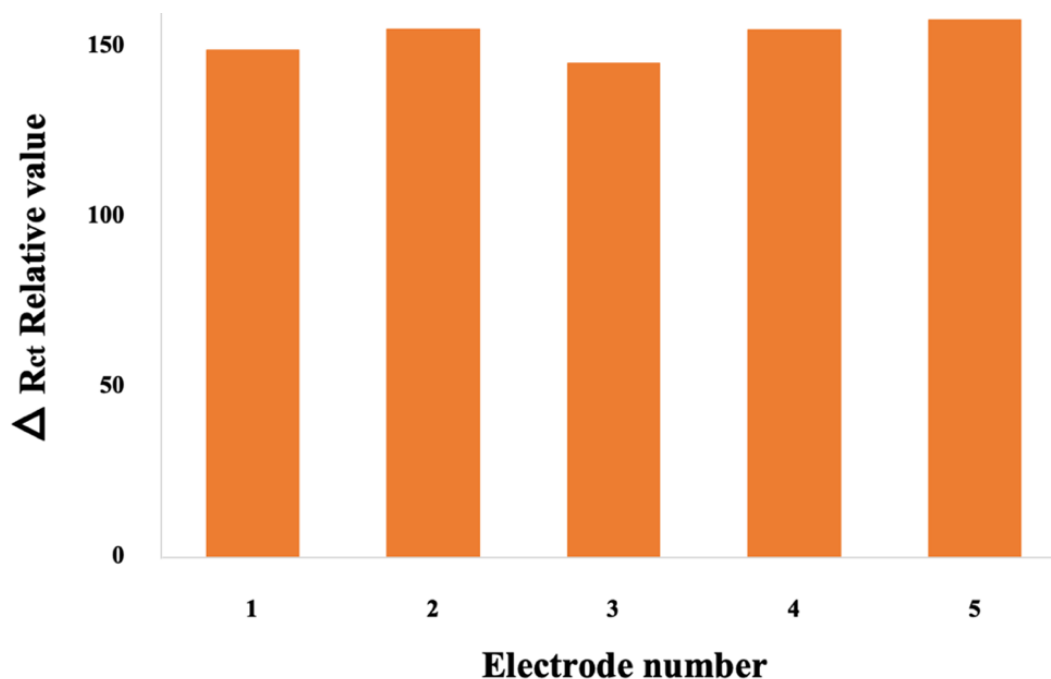


Figure 3.12 Response of the five developed immunosensors to detect 100 cells/mL of MCF-7 cells in the solution of 10 mM $[\text{Fe}(\text{CN})_6]^{3-/4-}$ containing 10 mM phosphate buffer at pH 7.0.

To summarize, the novel developed immunosensor discovered that modified streptavidin protein (normally known as the insulating layer) on the sensor surface, which contains PANI and AuNPs, showed no reduction in sensor conductivity. Additionally, as previously mentioned, streptavidin protein provided an improvement in the current signal of the developed immunosensor by collaborating with PANI and AuNPs. Here, our immunosensor (BSA/b-EpCAM/SA/AuNPs/PANI/SPAuE) was compared to other electrochemical biosensors for MCF-7 cells detection, as shown in Table 2. As can be seen, our immunosensor provided a wider linear range than previous research. Interestingly, the high sensitivity of our developed immunosensor achieved a limit of detection as low as 2 cells/mL, which is lower than the previous reports in Table 2. Thus, our developed immunosensor could be a promising tool for use to detect CTCs at various stages of cancer metastasis, from the early stages to the later stages.

Table 2 A comparative performance of different modified electrode strategies for breast cancer cell detection

Immobilization step	Electrochemical detection	Target	Linearity	Detection limit (cell/mL)	References
SYL3C- nanopropes/target/MCH/SYL3C/AuNPs/GCE	DPV	MCF-7	5×10^1 to 1×10^7	34	[109]
dsDNA-Ab ₂ /target/BSA/AuNCs+MWCNTs+ Ab ₂ /3DGF/GCE	DPV	MCF-7	1×10^2 to 1×10^6	80	[110]
target/Mt-HAS NCs/PGE	EIS	MCF-7	1.5×10^2 to 7.5×10^6	148	[111]
EpCAM+HRP+AuNPs/target/m-aptamer/MCH/CDT/PD/AuE	CV	MCF-7	1×10^2 to 5×10^4	5	[112]
target/BSA/b-EpCAM/SA/AuNPs/PANI/SPAuE	EIS	MCF-7	1×10^1 to 1×10^5	2	Our work

Note:

- GCE : glassy carbon electrode
- AuNPs : gold nanoparticles
- SYL3C : anti-EpCAM aptamer
- MCH : 6-mercaptop-1-hexanol
- 3DGF : 3D graphene
- Ab : antibody
- MWCNTs : multiwalled carbon nanotubes
- AuNCs : gold nanocages
- BSA : bovine serum albumin
- dsDNA : double-stranded DNA
- AuE : gold electrode
- PD : primer DNA
- CDT : circular DNA template
- m-aptamer : multivalent aptamer
- HRP : horseradish peroxidase
- EpCAM : epithelial cell adhesion molecules

CHAPTER 4

CONCLUSIONS

This study presented the success of a novel electrochemical immunosensor based on the contribution of both polyaniline and gold nanoparticles. The combination of polyaniline and gold nanoparticles could contribute to the sensor performances for detecting MCF-7 cells showing a limit of detection of 2 cells/mL. The developed immunosensor exhibited high selectivity to EpCAM antigen on the cancer cell surface. The immunosensor for detecting MCF-7 cells in the range of 10 to 10^6 cells/mL was accomplished. Furthermore, the immunosensor obtained satisfactory reproducibility in fabricated immunosensor. The performance of our developed immunosensor for CTC was compared to other studies for MCF-7 detection. Our immunosensor provided a wider linear range and the lowest limit of detection. It could be concluded that the developed immunosensor could be used as a potential tool for highly sensitive and selective quantification of MCF-7 cells in cancer patients for point-of-care CTCs detection. However, although the detection limit of this developed immunosensor is very low, the amount of CTCs in early-stage cancer patients was extremely low, with only 2-3 cells in 1 mL of a blood sample. It makes detection difficult when only an immunosensor is used. In future work, our developed immunosensor could be tested for the performance of CTCs detection in blood samples. Also, it is possible to combine the developed immunosensor with microfluidic technology for CTC isolation by controlling the fluid flow of a patient's blood sample into the measuring zone of immunosensor. Therefore, the combination of both technologies will increase the performance of CTC detection with more effectiveness in the future. Additionally, we hope that this immunosensor will enhance the chances of cancer patients recovering from the disease.

REFERENCES

- [1] Information of cancer disease from World Health Organization (WHO). [cited 25 Dec 2021]. Available from: <https://www.who.int/news-room/fact-sheets/detail/cancer>
- [2] Ferlay J, Ervik M, Lam F, Colombet M, Mery L, Piñeros M, et al. (2020). Global Cancer Observatory: Cancer Today. Lyon: International Agency for Research on Cancer.
- [3] Seyfried, T. N., & Huysentruyt, L. C. (2013). On the origin of cancer metastasis. *Critical reviews in oncogenesis*, 18(1-2).
- [4] Paterlini-Brechot, P., & Benali, N. L. (2007). Circulating tumor cells (CTC) detection: clinical impact and future directions. *Cancer letters*, 253(2), 180-204.
- [5] Farace, F., Massard, C., Vimond, N., Drusch, F., Jacques, N., Billiot, F., ... & Le Moulec, S. (2011). A direct comparison of CellSearch and ISET for circulating tumour-cell detection in patients with metastatic carcinomas. *British journal of cancer*, 105(6), 847-853.
- [6] Riethdorf S, Fritsche H, Müller V, Rau T, Schindlbeck C, Rack B, Janni W, Coith C, Beck K, Jänicke F, Jackson S. (2007). Detection of circulating tumor cells in peripheral blood of patients with metastatic breast cancer: a validation study of the CellSearch system. *Clinical cancer research*. 2007 Feb 1;13(3):920-8.
- [7] Nagrath, S., Sequist, L. V., Maheswaran, S., Bell, D. W., Irimia, D., Utkus, L., ... & Ryan, P. (2007). Isolation of rare circulating tumour cells in cancer patients by microchip technology. *Nature*, 450(7173), 1235-1239.
- [8] Grieshaber, D., MacKenzie, R., Vörös, J., & Reimhult, E. (2008). Electrochemical biosensors-sensor principles and architectures. *Sensors*, 8(3), 1400-1458.
- [9] Saberi, R. S., Shahrokhian, S., & Marrazza, G. (2013). Amplified electrochemical DNA sensor based on polyaniline film and gold nanoparticles. *Electroanalysis*, 25(6), 1373-1380.
- [10] Sassolas, A., Blum, L. J., & Leca-Bouvier, B. D. (2012). Immobilization strategies to develop enzymatic biosensors. *Biotechnology advances*, 30(3), 489-511.
- [11] Boffetta P, & Hainaut P. (2019). Encyclopedia of cancer. 3rd ed. Oxford (p. 299 –310.). Academic Press.

- [12] Beijer, N., Jager, A., & Sleijfer, S. (2015). Circulating tumor cell enumeration by the CellSearch system: the clinician's guide to breast cancer treatment?. *Cancer treatment reviews*, 41(2), 144-150.
- [13] Alix-Panabières, C., & Pantel, K. (2013). Circulating tumor cells: liquid biopsy of cancer. *Clinical chemistry*, 59(1), 110-118.
- [14] Paterlini-Brechot, P., & Benali, N. L. (2007). Circulating tumor cells (CTC) detection: clinical impact and future directions. *Cancer letters*, 253(2), 180-204.
- [15] National Cancer Institute. "Lung cancer". [cited 05 Apr 2022]. Available from: <https://www.cancer.gov/types/mesothelioma/patient/mesothelioma-treatment-pdq>
- [16] National Cancer Institute. "Biopsy, bone marrow aspiration and child". [cited 05 Apr 2022]. Available from: <https://visualsonline.cancer.gov/details.cfm?imageid=10187>
- [17] The foundation for gender special medicine. "Liquid Biopsy—Changing How We Diagnose and Treat Cancer". [cited 05 Apr 2022]. Available from: <https://gendermed.org/liquid-biopsy-changing-diagnose-treat-cancer/>
- [18] Kim, E. S., Hirsh, V., Mok, T., Socinski, M. A., Gervais, R., Wu, Y. L., ... & Sun, Y. (2008). Gefitinib versus docetaxel in previously treated non-small-cell lung cancer (INTEREST): a randomised phase III trial. *The Lancet*, 372(9652), 1809-1818.
- [19] Brock, G., Castellanos-Rizaldos, E., Hu, L., Coticchia, C., & Skog, J. (2015). Liquid biopsy for cancer screening, patient stratification and monitoring. *Transl Cancer Res*, 4(3), 280-290.
- [20] Diaz Jr, L. A., & Bardelli, A. (2014). Liquid biopsies: genotyping circulating tumor DNA. *Journal of clinical oncology*, 32(6), 579.
- [21] Diehl, F., Li, M., Dressman, D., He, Y., Shen, D., Szabo, S., ... & Kinzler, K. W. (2005). Detection and quantification of mutations in the plasma of patients with colorectal tumors. *Proceedings of the National Academy of Sciences*, 102(45), 16368-16373.
- [22] Diehl, F., Schmidt, K., Choti, M. A., Romans, K., Goodman, S., Li, M., ... & Kinzler, K. W. (2008). Circulating mutant DNA to assess tumor dynamics. *Nature medicine*, 14(9), 985.
- [23] Miller, M. C., Doyle, G. V., & Terstappen, L. W. (2010). Significance of circulating tumor cells detected by the CellSearch system in patients with metastatic breast colorectal and prostate cancer. *Journal of oncology*, 2010.

- [24] Yap, T. A., Lorente, D., Omlin, A., Olmos, D., & De Bono, J. S. (2014). Circulating tumor cells: a multifunctional biomarker. *Clinical Cancer Research*, 20(10), 2553-2568.
- [25] Sakamoto, S., & Kyprianou, N. (2010). Targeting anoikis resistance in prostate cancer metastasis. *Molecular aspects of medicine*, 31(2), 205-214.
- [26] Kirfel, G., Rigort, A., Borm, B., & Herzog, V. (2004). Cell migration: mechanisms of rear detachment and the formation of migration tracks. *European journal of cell biology*, 83(11), 717-724.
- [27] Nicolazzo, C., Gradilone, A., Loreni, F., Raimondi, C., & Gazzaniga, P. (2019). EpCAM low Circulating Tumor Cells: Gold in the Waste. *Disease Markers*, 2019.
- [28] Huebner, H., Fasching, P. A., Gumbrecht, W., Jud, S., Rauh, C., Matzas, M., ... & Ruebner, M. (2018). Filtration based assessment of CTCs and CellSearch® based assessment are both powerful predictors of prognosis for metastatic breast cancer patients. *BMC cancer*, 18(1), 1-8.
- [29] Wu, J., & Gu, M. (2011). Microfluidic sensing: state of the art fabrication and detection techniques. *Journal of biomedical optics*, 16(8), 080901.
- [30] Maheswaran, S., Sequist, L. V., Nagrath, S., Ulkus, L., Brannigan, B., Collura, C. V., ... & Digumarthy, S. (2008). Detection of mutations in EGFR in circulating lung-cancer cells. *New England Journal of Medicine*, 359(4), 366-377.
- [31] Stott, S. L., Hsu, C. H., Tsukrov, D. I., Yu, M., Miyamoto, D. T., Waltman, B. A., ... & Floyd, F. P. (2010). Isolation of circulating tumor cells using a microvortex-generating herringbone-chip. *Proceedings of the National Academy of Sciences*, 107(43), 18392-18397.
- [32] Strehlitz, B., Nikolaus, N., & Stoltenburg, R. (2008). Protein detection with aptamer biosensors. *Sensors*, 8(7), 4296-4307.
- [33] Mehrotra, P. (2016). Biosensors and their applications—A review. *Journal of oral biology and craniofacial research*, 6(2), 153-159.
- [34] Sawant, S. N. (2017). Development of biosensors from biopolymer composites. In *Biopolymer composites in electronics* (pp. 353-383). Elsevier.
- [35] Goode, J. A., Rushworth, J. V. H., & Millner, P. A. (2015). Biosensor regeneration: a review of common techniques and outcomes. *Langmuir*, 31(23), 6267-6276.
- [36] Aydin, E. B., Aydin, M., & Sezgintürk, M. K. (2019). Advances in electrochemical immunosensors. *Advances in clinical chemistry*, 92, 1-57.

- [37] Marazuela, M., & Moreno-Bondi, M. (2002). Fiber-optic biosensors—an overview. *Analytical and bioanalytical chemistry*, 372(5), 664-682.
- [38] Moina, C., & Ybarra, G. (2012). Fundamentals and applications of immunosensors. *Advances in immunoassay technology*, 65-80.
- [39] Zhang, Z., Cong, Y., Huang, Y., & Du, X. (2019). Nanomaterials-based electrochemical immunosensors. *Micromachines*, 10(6), 397.
- [40] Mollarasouli, F., Kurbanoglu, S., & Ozkan, S. A. (2019). The role of electrochemical immunosensors in clinical analysis. *Biosensors*, 9(3), 86.
- [41] Daniels, J. S., & Pourmand, N. (2007). Label-free impedance biosensors: Opportunities and challenges. *Electroanalysis: An International Journal Devoted to Fundamental and Practical Aspects of Electroanalysis*, 19(12), 1239-1257.
- [42] Elgrishi, N., Rountree, K. J., McCarthy, B. D., Rountree, E. S., Eisenhart, T. T., & Dempsey, J. L. (2018). A practical beginner's guide to cyclic voltammetry. *Journal of chemical education*, 95(2), 197-206.
- [43] Fu, J., Yao, Y., An, X., Wang, G., Guo, Y., Sun, X., & Li, F. (2020). Voltammetric determination of organophosphorus pesticides using a hairpin aptamer immobilized in a graphene oxide-chitosan composite. *Microchimica Acta*, 187(1), 1-8.
- [44] Chen, Z., Lv, H., Zhu, X., Li, D., Zhang, S., Chen, X., & Song, Y. (2014). Electropolymerization of aniline onto anodic WO₃ film: an approach to extend polyaniline electroactivity beyond pH 7. *The Journal of Physical Chemistry C*, 118(47), 27449-27458.
- [45] Ma, Y., Di, J., Yan, X., Zhao, M., Lu, Z., & Tu, Y. (2009). Direct electrodeposition of gold nanoparticles on indium tin oxide surface and its application. *Biosensors and Bioelectronics*, 24(5), 1480-1483.
- [46] Chooto, P. (2019). Cyclic voltammetry and its applications. In *Voltammetry* (p. 1). IntechOpen.
- [47] Deroco, P. B., de Fátima Giarola, J., Júnior, D. W., Lorga, G. A., & Kubota, L. T. (2020). based electrochemical sensing devices. In *Comprehensive analytical chemistry* (Vol. 89, pp. 91-137). Elsevier.
- [48] Scholz, F. (2015). Voltammetric techniques of analysis: the essentials. *ChemTexts*, 1(4), 1-24.
- [49] Lisdat, F., & Schäfer, D. (2008). The use of electrochemical impedance spectroscopy for biosensing. *Analytical and bioanalytical chemistry*, 391(5), 1555-1567.

- [50] Electrochemistry, P., Elements, C., Equivalent, C., & Models, C. (2010). Basics of electrochemical impedance spectroscopy. *Appl. Note AC*, 286(1), R491-7.
- [51] An, L., Wang, G., Han, Y., Li, T., Jin, P., & Liu, S. (2018). Electrochemical biosensor for cancer cell detection based on a surface 3D micro-array. *Lab on a Chip*, 18(2), 335-342.
- [52] Wang, R., Di, J., Ma, J., & Ma, Z. (2012). Highly sensitive detection of cancer cells by electrochemical impedance spectroscopy. *Electrochimica Acta*, 61, 179-184.
- [53] Shen, H., Yang, J., Chen, Z., Chen, X., Wang, L., Hu, J., ... & Feng, W. (2016). A novel label-free and reusable electrochemical cytosensor for highly sensitive detection and specific collection of CTCs. *Biosensors and Bioelectronics*, 81, 495-502.
- [54] Nezakati, T., Seifalian, A., Tan, A., & Seifalian, A. M. (2018). Conductive polymers: opportunities and challenges in biomedical applications. *Chemical reviews*, 118(14), 6766-6843.
- [55] Arshak, K., Velusamy, V., Korostynska, O., Oliwa-Stasiak, K., & Adley, C. (2009). Conducting polymers and their applications to biosensors: emphasizing on foodborne pathogen detection. *IEEE Sensors journal*, 9(12), 1942-1951.
- [56] Singh, R., Verma, R., Sumana, G., Srivastava, A. K., Sood, S., Gupta, R. K., & Malhotra, B. D. (2012). Nanobiocomposite platform based on polyaniline-iron oxide-carbon nanotubes for bacterial detection. *Bioelectrochemistry*, 86, 30-37.
- [57] Shoaie, N., Forouzandeh, M., & Omidfar, K. (2018). Voltammetric determination of the Escherichia coli DNA using a screen-printed carbon electrode modified with polyaniline and gold nanoparticles. *Microchimica Acta*, 185(4), 1-9.
- [58] Beygisangchin, M., Abdul Rashid, S., Shafie, S., Sadrolhosseini, A. R., & Lim, H. N. (2021). Preparations, Properties, and Applications of Polyaniline and Polyaniline Thin Films—A Review. *Polymers*, 13(12), 2003.
- [59] Yazdanpanah, A., Ramedani, A., Abrishamkar, A., Milan, P. B., Moghadan, Z. S., Chauhan, N. P. S., ... & Mozafari, M. (2019). Synthetic route of PANI (V): Electrochemical polymerization. In *Fundamentals and Emerging Applications of Polyaniline* (pp. 105-119). Elsevier.
- [60] Fomo, G., Waryo, T., Feleni, U., Baker, P., & Iwuoha, E. (2019). Electrochemical Polymerization. *Functional Polymers; Jafar Mazumder, MA, Sheardown, H., Al-Ahmed, A., Eds*, 105-131.

- [61] Korent, A., Soderžnik, K. Ž., Šturm, S., & Rožman, K. Ž. (2020). A correlative study of polyaniline electropolymerization and its electrochromic behavior. *Journal of The Electrochemical Society*, 167(10), 106504.
- [62] Jadoun, S., Verma, A., & Arif, R. (2021). Green synthesis of nanomaterials for textile applications. In *Green Chemistry for Sustainable Textiles* (pp. 315-324). Woodhead Publishing.
- [63] Pingarrón, J. M., Yanez-Sedeno, P., & González-Cortés, A. (2008). Gold nanoparticle-based electrochemical biosensors. *Electrochimica Acta*, 53(19), 5848-5866.
- [64] Yanez-Sedeno, P., & Pingarron, J. M. (2005). Gold nanoparticle-based electrochemical biosensors. *Analytical and bioanalytical chemistry*, 382(4), 884-886.
- [65] Arun Sharma and Vepa Kameswara Rao, 2020. Synthetic Applications of Gold Nanoparticles in Research Advancement of Electrochemical Immunosensors. *Trends in Applied Sciences Research*, 15: 151-167.
- [66] Liu, F., Zhang, J. Z., & Mei, Y. (2016). The origin of the cooperativity in the streptavidin-biotin system: A computational investigation through molecular dynamics simulations. *Scientific reports*, 6(1), 1-11.
- [67] Weber, P. C., Ohlendorf, D. H., Wendoloski, J. J., & Salemme, F. R. (1989). Structural origins of high-affinity biotin binding to streptavidin. *Science*, 243(4887), 85-88.
- [68] Taylor, C. R., Shi, S. R., Barr, N. J., & Wu, N. (2013). Techniques of immunohistochemistry: principles, pitfalls, and standardization. *Diagnostic immunohistochemistry*, 2, 1-42
- [69] Nguyen, T. T., Sly, K. L., & Conboy, J. C. (2012). Comparison of the energetics of avidin, streptavidin, neutrAvidin, and anti-biotin antibody binding to biotinylated lipid bilayer examined by second-harmonic generation. *Analytical chemistry*, 84(1), 201-208.
- [70] Wang, S., Hossain, M. Z., Han, T., Shinozuka, K., Suzuki, T., Kuwana, A., & Kobayashi, H. (2020). Avidin–biotin technology in gold nanoparticle-decorated graphene field effect transistors for detection of biotinylated macromolecules with ultrahigh sensitivity and specificity. *ACS omega*, 5(46), 30037-30046.
- [71] Dundas, C. M., Demonte, D., & Park, S. (2013). Streptavidin–biotin technology: improvements and innovations in chemical and biological applications. *Applied microbiology and biotechnology*, 97(21), 9343-9353.

- [72] Lu, X. Y., Wu, D. C., Li, Z. J., & Chen, G. Q. (2011). Polymer nanoparticles. *Progress in molecular biology and translational science*, 104, 299-323.
- [73] Otieno, B. A., Krause, C. E., & Rusling, J. F. (2016). Bioconjugation of antibodies and enzyme labels onto magnetic beads. *Methods in enzymology*, 571, 135-150.
- [74] Baeuerle, P. A., & Gires, O. (2007). EpCAM (CD326) finding its role in cancer. *British journal of cancer*, 96(3), 417-423.
- [75] Liao, M. Y., Lai, J. K., Kuo, M. Y. P., Lu, R. M., Lin, C. W., Cheng, P. C., ... & Wu, H. C. (2015). An anti-EpCAM antibody EpAb2-6 for the treatment of colon cancer. *Oncotarget*, 6(28), 24947.
- [76] Cimino, A., Halushka, M., Illei, P., Wu, X., Sukumar, S., & Argani, P. (2010). Epithelial cell adhesion molecule (EpCAM) is overexpressed in breast cancer metastases. *Breast cancer research and treatment*, 123(3), 701-708.
- [77] Ni, J., Cozzi, P. J., Duan, W., Shigdar, S., Graham, P. H., John, K. H., & Li, Y. (2012). Role of the EpCAM (CD326) in prostate cancer metastasis and progression. *Cancer and Metastasis Reviews*, 31(3), 779-791.
- [78] Liao, M. Y., Kuo, M. Y. P., Lu, T. Y., Wang, Y. P., & Wu, H. C. (2015). Generation of an anti-EpCAM antibody and epigenetic regulation of EpCAM in colorectal cancer. *International journal of oncology*, 46(4), 1788-1800.
- [79] Riethdorf, S., O'Flaherty, L., Hille, C., & Pantel, K. (2018). Clinical applications of the CellSearch platform in cancer patients. *Advanced drug delivery reviews*, 125, 102-121.
- [80] Cetin, D., Okan, M., Bat, E., & Kulah, H. (2020). A comparative study on EpCAM antibody immobilization on gold surfaces and microfluidic channels for the detection of circulating tumor cells. *Colloids and Surfaces B: Biointerfaces*, 188, 110808.
- [81] Czaplicka, M., Niciński, K., Nowicka, A., Szyborski, T., Chmielewska, I., Trzcńska-Danielewicz, J., ... & Kamińska, A. (2020). Effect of varying expression of EpCAM on the efficiency of CTCs detection by SERS-based immunomagnetic optofluidic device. *Cancers*, 12(11), 3315.
- [82] Desimoni, E., & Brunetti, B. (2013). Presenting analytical performances of electrochemical sensors. Some suggestions. *Electroanalysis*, 25(7), 1645-1651.

- [83] Miller, J., & Miller, J. C. (2018). *Statistics and chemometrics for analytical chemistry*. Pearson education. 6th ed. ISBN 978-0-273-73042-2
- [84] Taverniers, I., De Loose, M., & Van Bockstaele, E. (2004). Trends in quality in the analytical laboratory. II. Analytical method validation and quality assurance. *TrAC Trends in Analytical Chemistry*, 23(8), 535-552.
- [85] AOAC International. (2012). Guidelines for Standard Method Performance Requirements (Appendix F). *AOAC Off. Methods Anal.*, 1-17.
- [86] Shrivastava, A., & Gupta, V. B. (2011). Methods for the determination of limit of detection and limit of quantitation of the analytical methods. *Chronicles of young scientists*, 2(1), 21-25.
- [87] Magnusson, B & Örnemark, U. (2014). The fitness for purpose of analytical methods: a laboratory guide to method validation and related topics. *Eurachem Guide*. 2nd ed. ISBN 978-91-87461-59-0.
- [88] Martowicz, A., Spizzo, G., Gastl, G., & Untergasser, G. (2012). Phenotype-dependent effects of EpCAM expression on growth and invasion of human breast cancer cell lines. *BMC cancer*, 12(1), 1-16.
- [89] Chen, L., Peng, M., Li, N., Song, Q., Yao, Y., Xu, B., ... & Ruan, P. (2018). Combined use of EpCAM and FR α enables the high-efficiency capture of circulating tumor cells in non-small cell lung cancer. *Scientific reports*, 8(1), 1-10.
- [90] Stojanović, I., Ruivo, C. F., Van Der Velden, T. J., Schasfoort, R., & Terstappen, L. W. (2019). Multiplex label free characterization of cancer cell lines using surface plasmon resonance imaging. *Biosensors*, 9(2), 70.
- [91] Nikhil, B., Pawan, J., Nello, F., & Pedro, E. (2016). Introduction to biosensors. *Essays Biochem*, 60(1), 1-8.
- [92] Shoaie, N., Forouzandeh, M., & Omidfar, K. (2017). Highly sensitive electrochemical biosensor based on polyaniline and gold nanoparticles for DNA detection. *IEEE Sensors Journal*, 18(5), 1835-1843.
- [93] An, L., Wang, G., Han, Y., Li, T., Jin, P., & Liu, S. (2018). Electrochemical biosensor for cancer cell detection based on a surface 3D micro-array. *Lab on a Chip*, 18(2), 335-342

- [94] El Aggadi, S., Loudiyi, N., Chadil, A., El Abbassi, Z., & El Hourch, A. (2020). Electropolymerization of aniline monomer and effects of synthesis conditions on the characteristics of synthesized polyaniline thin films. *Mediterranean Journal of Chemistry*, 10(2), 138-145.
- [95] Korent, A., Soderžnik, K. Ž., Šturm, S., & Rožman, K. Ž. (2020). A correlative study of polyaniline electropolymerization and its electrochromic behavior. *Journal of The Electrochemical Society*, 167(10), 106504.
- [96] Fomo, G., Waryo, T., Feleni, U., Baker, P., & Iwuoha, E. (2019). Electrochemical polymerization. *Functional Polymers; Jafar Mazumder, MA, Sheardown, H., Al-Ahmed, A., Eds*, 105-131.
- [97] Yazdanpanah, A., Ramedani, A., Abrishamkar, A., Milan, P. B., Moghadan, Z. S., Chauhan, N. P. S., ... & Mozafari, M. (2019). Synthetic route of PANI (V): Electrochemical polymerization. In *Fundamentals and Emerging Applications of Polyaniline* (pp. 105-119). Elsevier.
- [98] Aldous, L., Silvester, D. S., Villagrán, C., Pitner, W. R., Compton, R. G., Lagunas, M. C., & Hardacre, C. (2006). Electrochemical studies of gold and chloride in ionic liquids. *New journal of chemistry*, 30(11), 1576-1583.
- [99] Etesami, M., Karoonian, F. S., & Mohamed, N. (2011). Electrochemical deposition of gold nanoparticles on pencil graphite by fast scan cyclic voltammetry. *Journal of the Chinese Chemical Society*, 58(5), 688-693.
- [100] Ongaro, M., Gambirasi, A., Favaro, M., Kuhn, A., & Ugo, P. (2014). Asymmetrical modification of carbon microfibers by bipolar electrochemistry in acetonitrile. *Electrochimica Acta*, 116, 421-428.
- [101] Prabhulkar, S., Tian, H., Wang, X., Zhu, J. J., & Li, C. Z. (2012). Engineered proteins: redox properties and their applications. *Antioxidants & redox signaling*, 17(12), 1796-1822.
- [102] Li, Y., Schluesener, H. J., & Xu, S. (2010). Gold nanoparticle-based biosensors. *Gold Bulletin*, 43(1), 29-41.
- [103] Hu, C., Dou, W., & Zhao, G. (2014). Enzyme immunosensor based on gold nanoparticles electroposition and Streptavidin-biotin system for detection of *S. pullorum* & *S. gallinarum*. *Electrochimica Acta*, 117, 239-245.

- [104] Yang, Z., Lan, Q., Li, J., Wu, J., Tang, Y., & Hu, X. (2017). Efficient streptavidin-functionalized nitrogen-doped graphene for the development of highly sensitive electrochemical immunosensor. *Biosensors and Bioelectronics*, *89*, 312-318.
- [105] Shen, H., Wang, C., Ren, C., Zhang, G., Zhang, Y., Li, J., ... & Yang, Z. (2020). A streptavidin-functionalized tin disulfide nanoflake-based ultrasensitive electrochemical immunosensor for the detection of tumor markers. *New Journal of Chemistry*, *44*(15), 6010-6014.
- [106] Zhang, B., Song, W., Pang, P., Lai, H., Chen, Q., Zhang, P., & Lindsay, S. (2019). Role of contacts in long-range protein conductance. *Proceedings of the National Academy of Sciences*, *116*(13), 5886-5891.
- [107] Shipps, C., Kelly, H. R., Dahl, P. J., Yi, S. M., Vu, D., Boyer, D., ... & Malvankar, N. S. (2021). Intrinsic electronic conductivity of individual atomically resolved amyloid crystals reveals micrometer-long hole hopping via tyrosines. *Proceedings of the National Academy of Sciences*, *118*(2), e2014139118.
- [108] Fischer, O., & Fischerová, E. (1995). Basic principles of voltammetry. In *Experimental Techniques in Bioelectrochemistry* (pp. 41-157). Birkhäuser, Basel.
- [109] Zheng, T., Zhang, Q., Feng, S., Zhu, J. J., Wang, Q., & Wang, H. (2014). Robust nonenzymatic hybrid nanoelectrocatalysts for signal amplification toward ultrasensitive electrochemical cytosensing. *Journal of the American Chemical Society*, *136*(6), 2288-2291.
- [110] Yang, Y., Fu, Y., Su, H., Mao, L., & Chen, M. (2018). Sensitive detection of MCF-7 human breast cancer cells by using a novel DNA-labeled sandwich electrochemical biosensor. *Biosensors and Bioelectronics*, *122*, 175-182.
- [111] Yaman, Y. T., Akbal, O., & Abaci, S. (2019). Development of clay-protein based composite nanoparticles modified single-used sensor platform for electrochemical cytosensing application. *Biosensors and Bioelectronics*, *132*, 230-237.
- [112] Yang, J., Li, X., Jiang, B., Yuan, R., & Xiang, Y. (2020). In situ-generated multivalent aptamer network for efficient capture and sensitive electrochemical detection of circulating tumor cells in whole blood. *Analytical chemistry*, *92*(11), 7893-7899.

VITAE

Name Mr. Hazim Samae

Student ID 6110320023

Educational Attainment

Degree	Name of Institute	Year of Graduation
Bachelor of Science (Applied Chemistry-Biology)	Prince of Songkla University	2017

Scholarship Awards during Enrolment

1. The student scholarship from Faculty of Medicine, Prince of Songkla University
2. The Graduate School, Prince of Songkla University awarded to Mr. Hazim Samae

List of Publication and Proceeding

Paper Samae, H., Thamphiwatana, S., & Phairatana, T. (2022). The Contribution of Polyaniline and Gold Nanoparticles for Enhancing Current Signals of Streptavidin Based Immunosensor. ECS Transactions, 107(1), 827.

(Submitted to ECS Transactions: Electrochemical Society)